10

MEMS-Based Sensing Systems: Architecture, Design, and Implementation

S. T. Amimoto,* A. J. Mason,† and K. Wise†

10.1 Introduction

The microelectronics industry has grown tremendously during the past few decades, largely because of increasing demand for microprocessors and memory. Advancements in microelectronics technology continue to meet the strong demand for more sophisticated and lower-cost electronics. In some areas of the industry, low-volume, custom ASICs (application-specific integrated circuits) are commonly being built to fulfill many of the world's electronic needs.

Rooted in microelectronics technology, microelectromechanical systems (MEMS)[1] has created a new industry of integrated sensors and actuators. MEMS technology has lowered the cost of these devices and opened new markets for MEMS transducers,[2] which will be increasingly important in providing a means for capturing information from the physical world and converting it to digital form.[3,4] As the MEMS industry grows, the trend is to combine transducers with increasingly sophisticated circuits[5–7] to form "smart" sensors. The low cost of signal-processing electronics (microprocessors, digital signal processors, etc.) makes it possible to join this circuitry with sensors[8] to form complete microsystems.

Microinstrumentation systems[9] that combine sensors, actuators, and signal processing circuitry on a common substrate are, in fact, now in development. These microsystems form autonomous units capable of gathering nonelectronic information, transducing the data to electrical signals, processing the information, making decisions based on it, and finally passing it on to other electronic systems that gain intelligence from the process.[10] Specifically for space applications, these functions may be used to monitor the environment experienced by a launch vehicle or satellite during assembly, transportation to launch site, storage, launch, and orbit. This information may be critical to aid identification of failure modes or anomalies during a failure investigation.

This chapter examines a MEMS-based data-logging system for a space application and presents two approaches to the development of multiparameter sensor (MPS) microsystems. The two microsystems have been designed as subsystems in vastly different macrosystems, yet they share many component-level functions and have similar goals. The first microsystem uses a "top-down" design approach: requirements of the macrosystem are established at the start. A survey of commercial components that may be used in an MPS system is provided to help the developer make choices for implementation. An implementation of this top-down system is described.

The second microsystem takes a "bottom-up" approach: requirements are largely determined by the needs of the transducers.The following topics are also covered.

- The architecture of the microsystem
- A review of current applicable MEMS technologies
- Design, fabrication, testing and calibration of the bottom-up-design microsystem
- Challenges faced during the design of each microsystem as sample procedures for MPS system development

*Mechanics and Materials Technology Center, The Aerospace Corporation, El Segundo, California

†Department of Electrical Engineering and Computer Science, University of Michigan

These two microsystems span a range of state-of-the-art design approaches, from those based on commercially available components to those based on advanced MEMS technologies. Designers can use these systems as guides to choose components and gain insight into the design and integration of an MPS system.

10.2 MEMS-Based Monitoring System for Space Applications

The European Space Agency Round-Table discussion[11] concludes that incentives to use micro/nanotechnology derive from its ability "to meet new or expanded flight performance requirements, recover from failure or a serious mission degradation event, increase reliability, and reduce overall system cost." MPS systems, for example, offer significant potential for decreasing the failure rates of U.S.-launched vehicle systems. Between 1984 and 1994, failure rates of DOD and non-DOD launches were 4.7% and 8.9% for 106 and 90 missions, respectively.[12] Of the 13 failures, five were attributed to the propulsion system. An MPS system can supply critical information to reduce delays in identifying the cause of a failure and to increase reliability and cost reductions on future flights.

On a Titan IV, one of the largest and best-instrumented launch vehicles, only 75 independent sensors can be monitored. Bandwidth restrictions, no data-processing, wires to each sensor, lack of small-sensor-form factors, and weight present severe limitations in the number of sensor locations that can be monitored. Some engine compartments are not monitored because of their distance from a central controller and difficulty in wiring. In addition, changing a sensor location/channel precipitates a significant analysis and qualification process that can cost up to $500,000. Small, low-cost, wireless, unobtrusive sensors could easily be moved without incurring this expensive process. These sensors will perform a large number of measurements at different locations, each fully instrumented with a set of sensors, and will lead to faster flight characterization of vehicle design and configuration. If these sensors preserve critical timing or phasing information, this would unambiguously identify where and when an abnormal event may have occurred.

Because of the low number of sensors and the high number of different flight-assembly configurations, the Titan IV-class launch vehicle has not been fully characterized despite its 10 years of flight history. Historically, data from each flight have indicated that the design margin was exceeded, often precipitating a study of design margin or requalification and testing to ensure that later flights will be successful. A single set of flight sensors costs $4 million without installation; furthermore, the hardware weighs 170 lb.[13] The fact that technology development has caused launch vehicles to evolve at a rate faster than they can be characterized is not unique to Titan. Only eight sensors are in use for the Delta rocket program, which suffered a spectacular failure on 17 January 1997 on flight K126.[14] A sizable effort was initiated to investigate potential causes of the failure. If the rocket had been instrumented with more sensor capability, the investigation may have been less costly.

MEMS-based sensors offer many advantages for the design of a multiparameter system for a launch-vehicle application. In particular, a "peel-and-stick" MEMS-based sensor system would have significant advantages over current flight environmental monitoring systems, including the following.

- Reliability is increased by a higher level of integration with a smaller chip count.
- Redundancy is made possible by low-cost sensors.
- Small-form factors result from the small sensor size and integration of supporting sensor electronics.
- Decreased size also leads to lower power consumption because of lower stray capacitance and thus a smaller battery requirement.

- With wireless chip sets, radio frequency (RF) or optical communications can reduce installation costs associated with conventional cables, a significant portion of the overall installation cost.
- With a microprocessor at each node, a networked MPS system offers capabilities far beyond merely reporting and routing data. Networking when combined with distributed intelligence will provide data compression, anomaly reporting, control or commanding operations, power management, transitions from one network mode to another, and various services such as error correction, time synchronization, data analysis, self-test, and autonomy.

The low cost of MEMS-based sensors enables their proliferation in many instrument or monitoring systems. As a result, data collection and node management become a paramount topic of concern. In very large node systems the cost drivers may not be the MEMS sensors, but the network data acquisition/management systems. On the other hand, without networking and other service capabilities, such as reliable reporting of high data rates from sensors such as accelerometers and acoustical devices, there becomes a need to incorporate autoconfiguration/modification protocols, which may in itself impede the proliferate use of sensors within a single system.

Advantages of an MPS system can be extended to military and commercial flights:

- It could readily carry out housekeeping on the Space Station by monitoring temperature, pressure, oxygen levels, and vibration and by detecting chemical vapors. (See Chapter 11).
- Monitoring Delta and other space-vehicle engines and satellite components in transport or storage could significantly improve reliability and increase confidence that they were not exposed to conditions exceeding their design or environmental specifications, a problem that has plagued nearly all satellite programs.
- An MPS system could assist NASA testing of a scaled version of a crew-return vehicle (CRV) to bring future Space-Station personnel back to Earth. The CRV is an unpowered but steerable reentry vehicle. The MPS system could monitor pressure and acceleration of the endo-atmospheric CRV flight tests being conducted at Edwards Air Force Base, California.
- A compact wireless version of an MPS system could have greatly facilitated data collection in ground testing of a newly fabricated Atlas payload transporter used to carry the payload for an Atlas rocket from its fairing encapsulation building to the launch pad. Test goals were to identify mode shapes and frequencies and to log peak acceleration events during a road test.

The number of space-related applications is growing, and the opportunities for the use of an environmental, data-logging MPS system are challenges awaiting system developers.

10.3 Macro System-Level Architecture

The macro-level architecture of an MPS is based on its requirements, availability of hardware and software, and the trade-offs facing the designer. These are discussed in the following sections.

10.3.1 Requirements for a Launch-Vehicle Multiparameter System

Discussion of the requirements that form the basis of a design for a multiparameter system will focus on the needs of an instrumentation system for the Titan IV, but may be extended to the space applications previously cited. Measurement parameters are taken from documentation of the Wideband Instrumentation System (WIS)[15] and Lift-off Instrumentation System (LOIS)[16] used on a Titan IV. These systems are based on hardwired sensors that are polled by a controller; the resulting digital data are formed into packets that are transmitted to ground using RF with a pulse-code modulated carrier at 2.2–2.4 GHz. Two unity-gain antennas, one on each side of the launch vehicle, are used in conjunction with a high-gain ground antenna. The vehicle is tracked to within a few degrees above the horizon, necessitating the use of an RF spectrum region that suffers little

atmospheric attenuation. The line-of-sight range is approximately 100 km. For the RF spectral region of 10 GHz and below, little attenuation is observed. Since maximum data rates are proportional to the carrier bandwidth, a sufficiently wide band near 10 GHz appears to be ideal.

A preliminary survey of the types of measurements employed by the WIS system is listed in Table 10.1. They are vibration, acoustic levels, acceleration, pressure, strain, and shock resulting from pyrotechnic firing events. Vibration and acoustics generally refer to the shaking that occurs due to the higher-frequency phenomena, such as turbulent flows across certain regions of the skin of the vehicle; acceleration refers to the lower frequency shaking and acceleration of the vehicle in the direction of motion. The bandwidths overlap as indicated in the table. The total launch event is 10 min, in contrast to the time spent to install the sensors (more than a week) and to await other vehicle preparation procedures (which can easily require a few months). The sensor system should be robust enough to accommodate the maximum amplitude and bandwidth level that a sensor might experience and to anticipate changes in the location of sensors without regard to the system's environmental qualification level. The measurement requirements and qualification levels may vary from location to location on the vehicle. The minimum and maximum temperature extremes to be encountered are −44 to +75°C,[17] a range readily met by most MEMS sensors.

Total raw data rates for the vehicle MPS system can be easily estimated:

$$\text{Measurement rate} = \sum_i \text{sensor rate}(i) \times \text{bandwidth}(i) \times \text{oversample factor}, \qquad (10.1)$$

where the summation is performed over all sensor types, i. For a given sensor it is unlikely that more than a single shock event will occur for the duration of the launch at a single location. Shock data may be acquired with a large bandwidth of 10 to 20 kHz, but its duration may be only 20 ms.

Table 10.1. Raw Characteristics and Requirements of an Environmental MPS System[18]

Measurement parameters (based on LOIS and WIS)[a] and sample rates at a single location (maximum amplitude values) • 3-axis vibration: 10–2000 Hz, ± 300-g max amplitude; 12 kHz • Acoustics: 10–4000 Hz, ± 185-dB max range; 8 kHz • Acceleration: 0–50 Hz, ± 10-g max amplitude; 100 Hz • Pressure: 0–50 Hz, 0–16-psia range; 100 Hz • Strain: 0–50 Hz, 900 min/in. or ± 2000 psi; 100 Hz • Number of sensor locations: 500 • Measurement time: 10 min • Shock event: 10 kHz for 0.02 s; 400 measurements/event • Elapsed time from installation to launch: several weeks to months
Communication: 2-way; range, ≥100 km; wireless 10-GHz telemetry band
Mountable with wire leads to specified attachment points as needed
Compact, low-weight, low-power form factor
Survivability and environmental parameters: vibration, shock, EMI, radiation, temperature, atmospheric to vacuum pressures, contamination resistant, humidity resistant
Self-configurable
Built-in test for installation and system health monitoring
Reliable data and system function

[a]LOIS: Lift-Off Instrumentation System, WIS: Wideband Instrumentation System

By using thresholding as a criterion to send data, the average data rate can easily be met by the communication system. Thresholding is a concept in which data may be measured but not acted upon unless a threshold value is exceeded. When this occurs, the data, for example, may be stored or reported as necessary. Thresholding acts as a filter to reduce the quantity of data while maintaining information and data quality. Data may need to be stored when aggregate peak data rates occur. The total raw data rate is calculated by summing over all sensor node rates:

$$\text{Total data rate} = \sum_{i} \text{sensor node rates } (i) \tag{10.2}$$

For the entire vehicle, total raw data rate acquired by all 500 nodes is 10 MHz. The bit rate is calculated from the total data rate. For a constant sample accuracy,

$$\text{Bit rate} = \text{total rate} \times (\text{bit accuracy} + \text{overhead}) \tag{10.3}$$

For data of 8-bit accuracy, we can assume 10 bits/sample (e.g., an additional 2 bits for parity checkbit and signbit) × 10 MHz, or 100 Mbits/s must be transmitted by the RF link to ground networking. Overhead for data packeting and error correction is neglected. The spectral efficiency of a communication system is often expressed by the ratio of the information carried per carrier-bandwidth frequency.

$$\text{Spectral efficiency} = \text{bit rate/carrier bandwidth} \tag{10.4}$$

Assuming a bandwidth of 200 MHz for the WIS, the spectral efficiency is 0.5 bits/s/Hz with no thresholding. This spectral efficiency is easily met by modern digital communication systems.[19] It is also assumed that some form of data compression will be used to reduce data transmission rates.

Sensor data below a certain threshold level will be of little value for anomaly resolution purposes unless there is assurance that the data reporting system is indeed functional. Otherwise the lack of data may indicate a nonfunctioning sensor or sensor node or other malfunctions. Thresholding while reducing data flow to "essential" data will introduce intermittent data reporting, which may be solved using time tagging. The nature of this effect may also depend on the flight profile, location of the sensor node, and the sensor type. In addition, data compression, such as that used by video compression schemes such as MPEG, JPEG, and Wavelet-based chip,[20] could also lead to intermittent data flow.

There may also be a latency reporting requirement. Latency can be defined as the time delay of the reporting system between time of measurement and the time these critical data are transmitted by the vehicle to the ground station. This time requirement can be set by considering the velocity at which a catastrophic phenomenon is able to propagate over a critical distance of the vehicle and to reach a component in the chain of the reporting system that will prevent critical data flow. One crude estimate of the maximum latency time may be derived from the distance of the edge of the solid-rocket booster to the center of the core vehicle, approximately 5 ft, and the speed of propagation of a blast wave at the speed of sound, 340 m/s, which yields a latency time of 4.5 ms.

A related issue concerns the nodes: unless there is confirmation that all nodes were functioning during the catastrophic event, no definitive conclusion can be made concerning the fidelity of the data. If data are not present, was the data amplitude below threshold or was the node not functional? Thus periodic confirmation of node integrity is needed if no data have recently been transmitted from that node. There will be significant value in the assurance that only a major vehicle anomaly could make the node nonfunctional.

Network self-configuration is an important feature for the launch-vehicle network and refers to the network's ability to organize itself. During installation, the configuration of the network architecture is changing. When the network is placed in active mode, the network configures itself by polling all nodes so that the master nodes will know which sensor nodes are within their compartments. Network self-configuration is also needed during the launch as each successive stage of the vehicle is ignited and then dropped off and the network undergoes a dynamic configuration change. Thus, self-configuration is an essential feature of the network architecture. For networking robustness, redundant network paths could be added to enable dynamic routing of messages and data around nodes that may have failed for whatever reasons.

Compartments where many sensors may be mounted are located throughout the launch vehicle and are shown in Fig. 10.1. The maximum compartment-to-compartment distance is between compartment 2A, where the transmitter for the telemetry system to the ground receiver is found, and compartment 1C at the base of the vehicle, a distance of 120 ft. The distance to the top of the payload fairing from compartment 2A is about 86 ft for the longest available payload fairing. These distances represent the maximum ranges for an RF transceiver on the vehicle. Distances within a compartment are typically on the order of 10 ft, where multiple-path reflections of RF signals may be anticipated because of extensive use of metal and the many vehicle parts. Outside the vehicle, relatively good lines of sight may be maintained, and little interference may be expected.

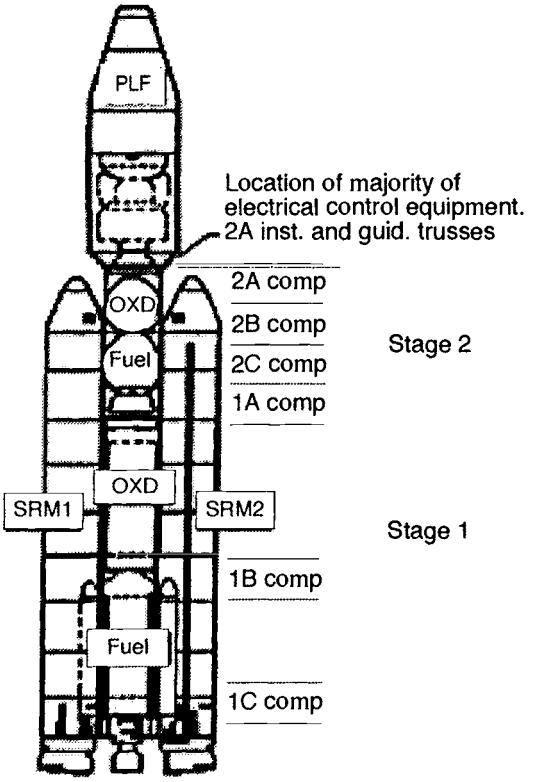

Fig. 10.1. Compartments of a Titan IV vehicle are labeled by stage numbers 1 or 2. Stage 1 uses the two outer solid-rocket motors and the lower liquid center-core stage. The second stage is liquid fueled. The length of the solid rockets is 112 ft, and the length of the payload fairing (PLF) is approximately 50–86 ft, depending on the upper stage and the payload configuration used.

10.3.2 Hardware/Protocols—Choices for MPS Implementation

Once requirements for a system are fixed, the designer must select specific implementations of hardware and software. Among various issues to be considered are performance specifications, amount of effort to integrate the many components into a system, networking protocols, the type of developmental tools, and whether the cost of the approach is within budget. The following surveys, primarily of commercial off-the-shelf (COTS) components, are provided to help the integrator developer with the many choices involved in this design. The components include sensors, microcontrollers, networking/device protocols, batteries, and communication devices.

10.3.2.1 Commercially Available Sensors

Surveys of available technologies provided a data base from which commercial sensors, accelerometers, and pressure sensors could be selected for the design of the MPS system. A large number of sensors are indeed available. Almost all sensors are in the form of sensing elements with analog output; very few are capable of providing direct digital output. Selection criteria required the sensors to be fabricated using MEMS methods. Examples of noncommercial sensors are discussed in Subsec. 10.6.3.

10.3.2.1.1 Commercial MEMS Accelerometers

A large number of accelerometers are commercially available, driven by the automobile airbag market. Results from a search of accelerometers and vendors are shown in Appendix 10. A at the end of this chapter. During the past year, accelerometer demand has outstripped production, resulting in temporary shortages. Competition from a large number of manufacturers has kept prices low. Individually packaged commercial COTS accelerometers in chip form may be purchased for as low as \$19–\$35 per sensor in small quantities (25 or below).

Accelerometer sensors are available in compact chip form or finished packaged assemblies with external mounting fixtures or environmental mounts and often with amplifier circuits. Some have customizable gain, offset settings, and printed circuit boards. The large weight and sizes of finished sensor packages relative to the internal die within are mostly associated with the final packaging, which addresses the interconnects and the physical integrity of the sensor package.[21] Thus repackaging of sensors with their supporting data-logging infrastructure, i.e., processors, memory, and communications, should lead to a significant reduction in weight and size of the completed package. These advantages are further discussed in Sec. 10.6.

10.3.2.1.2 Survey of MEMS Pressure Sensors

Pressure sensors produced by nano/micro fabrication techniques were surveyed. Many are available in 8-pin DIP packages. An abbreviated list of the sensors surveyed is shown in Table 10.2, which also lists only a few of the many configurations. In general, these sensors use the mechanism of the deformation of a membrane that is sensed by a strain gauge patterned on the membrane. Capacitive pressure sensors have been fabricated, as discussed in Subsec. 10.6.3.1. These gauges are incorporated into a Wheatstone bridge to produce an analog voltage change as a function of pressure. The table is intentionally short and does not reflect the wide variations in features that manufacturers offer. A summary of the findings follows.

- Some vendors offer versions that provide a buffer amplifier with adjustable gain.
- Some models incorporate a small tube to allow a connection to a pressure or vacuum tube.
- Chips from different vendors are often pin-for-pin identical, reflecting the level of competition.
- Pressure is usually sensed through a small hole on the chip.
- Power is typically under 150 mW.

Table 10.2. Typical MEMS Pressure Sensors for Low-Pressure Applications

Vendor	Model No.	Supply Voltage (V)	Input Range (psia)	Size / Weight (in., in., in./g)[a]	Power (mW)	Cost ($)
IC Sensors[b]	1431-015-A	3	0–15	0.3, 0.3, 0.14/0.30	2.0	20.0
Si Microstructures[c]	5310-015-A-P	5	0–15	0.3, 0.3, 0.14/0.30	7.5	12.5
Lucas Nova Sensors[d]	NPC-410-015-3L	3–15	0–15	0.3, 0.3, 0.14/0.25	7.5	20.0

[a]Dimensions in inches, mass in grams.
[b]EG&G IC Sensors, Milpitas, California
[c]Silicon Microstructures, Fremont, California
[d]Lucas Nova Sensors, Fremont, California

- Bandwidth can be as high as 1 kHz.
- Gauges are available with full-scale pressure ranges from 0.15 to 4000 psi.
- Pressure sensors are available in many models reflecting the attachment interface, compatibility with fluids under measurement, and electronic mounting options such as surface, DIP, and transistor cans.
- Prices (as of 1997) are often under $20 each in low quantities.

10.3.2.2 Survey of Microcontrollers and Data-Logging Systems

Output from most sensors is analog voltage. These signals must be converted to digital form using analog-to-digital converters (ADCs) and ported into a processor for calibration, time stamping, thresholding, and data compression, using the application software. The processor must also perform networking services, such as communication-media access, time synchronization across the networked sensors, formation of data packets, network configuration control, autonomous configuration control of network nodes, and packet routing. These functions are often implemented in hardware called a microcontroller, generally a combination of an ADC and a processor. Some of the microcontroller's more significant attributes for a designer include power consumption during active and sleep modes, processing speed, flash memory (EEPROM) or program memory, number of ADC channels, form factor, number and type of communication ports, communication rates, and hardware/software support by the vendor.

All the controllers listed in Appendix 10.B (at the end of this chapter) are relatively small and have a correspondingly small power appetite. The table is not a complete listing, but rather includes representative devices available to system developers. Some entries are also stand-alone data-logging systems, such as, the PC 104, the TattleTale 8, the Honeywell TSMD, the University of Michigan Microcluster, and the Adcon Telemetry m-T device. Of these, the smallest COTS system is the m-T, useful for low-data-rate, low-power applications. The others are microcontrollers with many of the attributes desired in a data-logging system. Using packaged chips or compact microcontroller cards considerably reduces the effort to develop an instrumentation node. Some noncommercial devices are also included, such as the Honeywell Time Stamp Measurement Device (TSMD), the University of Michigan Microcluster Watch, and the Air Force Research Laboratory Advanced Instrumentation Controller (AIC), as examples of the direction and the state of the art in advanced microcontroller/data-logging designs. The University of Michigan Microcluster is discussed in detail in Secs. 10.6 and 10.7.

Device characteristics are highly variable. Physically, the largest data-logger system is the PC104 with a maximum dimension of 90 mm. The smallest is the University of Michigan Microcluster with a volume of 5 cc for the complete system of processor, sensors, and communication. Peak power consumption is also quite large for the PC 104 processor at 10 W compared to 50 mW for the AIC. The number of ADC inputs varies from 4 to 10, with sampling rates from 8 to 100 kHz. The number of I/O ports for communication and memory varies from 1 to 6. Finally, environmental specifications for each device in meeting a space application also vary. One will be used for deep space, and others have been flown in Shuttle missions. All space missions require meeting launch vibration specifications and a minimum level of radiation hardness.

The Apple Newton using the ARM processor is included because of the processor's high figure of merit for mobile computing, expressed as a ratio of processing capacity to power consumption. With a high figure of merit, a smaller battery size can meet mission processing requirements. In principle, despite the processor's high clock rate and processing power, optimizing clock speed can optimize processor power for each application. In general, electrical power scales with the clock speed for each processor. However, the corollary is not necessarily true, meaning processors of high maximum processing power do not automatically use higher electrical power. Future low-power networked processors will very likely share similar characteristics with the ARM processor where networking overhead must be supported.

10.3.2.3 Software/Networking Protocols

Software/networking selection is often determined by a number of criteria:

- Desired computational and networking tasks
- Language and quality of the library that supports the available processor
- Availability of such fundamental software as device drivers
- Level of implementation of networking and networking services
- Availability of technical support and services by vendors
- Ease of use determined by diagnostic tools and development time and tools.

Another motivating selection criterion is the extreme reluctance of a user to redevelop the software for networking control, especially if it is already implemented for a processor. Standardized software that drives networks is needed for open networking systems.[22] Hardware is explicitly configured for networking,[23] and includes LonWorks[24] and Controller Area Network (CAN).* Each is briefly discussed with few details. Most are intended to be used with wired buses.

The LonWorks consortium offers networking hardware and software. The neuron-node hardware provides all layers of networking but one, as implemented by a media-access CPU and a network CPU, which allows the user to concentrate primarily on the application layer in an application CPU. All CPUs are combined in a single Neuron chip. The protocol is an accepted standard for ASHRAE BACnet North American building automation standard, adopted by the European Forecourt Standards Forum for European fuel stations and accepted by the American Association of Railroads for pneumatic braking.

The Neuron chip requires 85 mW of power, and the application layer is programmed in the Neuron-C language. Compatible communications media, such as wired or wireless transceivers, are available from vendors, as are developmental tools for nodes or systems and network service tools. Available gateways, routers, repeaters, and network interfaces allow for multiple media use and connecting hosts. In addition, a portable LonTalk protocol is available royalty free for imple-

*See Internet sites <http://www.nrtt.demon.co.uk>, <http://www.dgtech.com>, and <http://www.kvaser.se> for CAN products.

mentation on any microprocessor. Typical messages or packets use 10 bytes/message; additional bytes may be added for more data. The LonWorks networking system is designed for low data rates, robust reliability, and control of network. High data rates can be accommodated using a faster communications medium or a separate communication applications layer. LonMark is a standard that has been adopted by a large industrial consortium that maintains interoperability between the hardware products, offers a means by which products can be interchanged, and maintains a plug-and-play integration even with custom-engineered components.

CAN is a shared broadcast bus with speeds up to 1 Mbits/s. The protocol comes in several flavors of differing levels of capability. It is based on sending messages or frames that can be varied in lengths of 0–8 bytes. The frame has an identifier that must be unique. The CPU for the more powerful FullCAN architecture can store several frames, updates the buffered frames, and marks them for transmission. If the identifier matches, the shared variable can then be examined. The object is to create a set of shared variables in the network. The CAN controllers available include Intel 82527, Phillips 82C200, NEC uPD72005, Siemens 81C90, and Motorola TOUCAN on 683XX devices. Developmental hardware is offered by numerous vendors.[24] Data rates on CAN are limited by the physical bus length and transit time necessary for error recovery. A bus length of up to 50 m is supported at 1 Mbit/s. A gate array implementation has been reported for a FullCAN Controller.*

10.3.2.4 Smart Transducers

Since 1993, industry and government have recognized the need to select a single, open, network-independent communication interface standard for smart transducers, where the transducer is defined as a sensor or an actuator. This ongoing effort in the United States is led by the Manufacturing Engineering Laboratory of the National Institute of Technology (NIST) and the Instrumentation and Measurement Society's Technical Committee on Sensor Technology TC-9 of the Institute of Electrical and Electronics Engineers (IEEE). The goal is to define a uniform approach to support multiple bus standards and to enable transition to most of the existing popular networks. The interface is digital, defines a standard transducer electronic data sheet (TEDS) and its data format, and defines an architecture with application software independent of protocol and technology. Smart transducers would be able to convert and process signals, compensate for environment, convert analog-to-digital or digital-to-analog signals, control logic, provide local memory (EEPROM), and identify themselves. Each transducer will be physically associated with TEDS.

Two draft standards for the Smart Transducer Interface† have been proposed, the Network Capable Application Processor Information Model, IEEE P1451.1, and the Transducer to Microprocessor Communication Protocol and Transducer Electronic Data Sheet, IEEE P1451.2. The benefit of the first standard is to provide a network-independent, neutral interface for the application processor. Once the application is developed by the vendor, the user would link the transducer application software with a driver library supplied by the vendor to enable a plug-and-play environment. To use the transducer with another network, the user would simply recompile and link with the library provided by the vendor. This concept of abstracting the application from hardware has been used successfully for Windows® and Postscript printers.

---

*Initec AG, Bielst. 10, CH-4104 Oberweil, Switzerland, ph +41-61-7169616.

†Both proposed smart transducer interface standards, P1451.1 and P1451.2, are available from the IEEE Standard Department, 455 HOES Lane, Piscataway, NJ 08855; telephone: 800.678.4333.

The second standard, IEEE P1451.2, describes the contents of TEDS, a digital hardware interface to access TEDS, read sensors, and set actuators. Measurement aspects are captured in a smart transducer interface module (STIM) and application-related aspects in a network-capable application. The interface allows for triggering of one or more transducers and a variable-date clock rate. A generic STIM consists of the transducer, signal conditioning, TEDS, and a microcontroller that implements the P1451.2 interface. TEDS, which describes the type of sensor, the operation, and the attributes of the transducer, is structured into five parts: meta, channel, calibration, application-specific, and extension. In meta-TEDS is the description of the data structure, worst-case timing, and channel-grouping data. In channel TEDS is the upper/lower range limits, physical units, warm-up time, existence of self-test capability, calibration mode, and trigger parameters. The calibration TEDS contains the calibration date, the calibration interval, and parameters for a multisegment model. The application-specific TEDS is self-evident, and the extension TEDS is used for future extensions.

STIM is hosted by a network through a network capable application processor (NCAP). The P1451.2 standard describes both the hardware and firmware interface residing in the NCAP side of the NCAP/STIM interface. This firmware includes the network protocol, the application firmware, and the STIM driver. Three network providers have developed IEEE 1451.2 drivers for the NCAPs, Allen-Bradley (DeviceNet), Echelon(LonWorks), and Honeywell Micro Switch (Smart Distributed System).

10.3.2.5 Power Supply

The primary energy source for many MPS systems will be batteries. "Primary" and "secondary" refer to low-cost commercial, single-use batteries and to rechargeable batteries, respectively. In the absence of permanent wires to provide power, other sources such as solar cells or RF power may be used for microsystems.

Battery attributes that designers must consider include voltage, capacity, energy density, size, cost, storage life, discharge current, degradation mode, and rechargeability. Recharging of secondary batteries must also consider current limits or temperature rise during charging and the source of this power. Other considerations include package reliability, lifetime limited by recharge cycles, operating temperatures, cell mortality, cell leakage current, etc. Batteries are available in a number of sizes and voltages. Cells must be stacked in series to achieve higher voltages. In addition, the discharge-voltage-versus-time curve must be considered, and appropriate power conditioning used to optimize stored-power utilization. If the cells show a continuous voltage drop during the discharge profile of the battery, then a switching regulator must be employed to preserve efficient conversion of stored energy to delivered energy at fixed voltages.[25] Up to 90% efficiencies are possible. For batteries that exhibit a flat discharge profile, a voltage regulator may be sufficient.

A brief summary of battery characteristics is shown in Table 10.3. Also, the 100% capacity rating for rechargeable batteries must be derated to allow for additional mass needed for the battery package surrounding the cells. These factors and the practice of not charging to full capacity to increase life cycle may reduce the energy/mass ratio by as much as a factor of five.[26] Since battery casing becomes a larger fraction of the mass as batteries become smaller, the derating factors likewise become higher. In general, lithium batteries have excellent energy densities but are only able to deliver power at low current. These will likely be the choice of a low-power MPS system. Higher current is possible for NiCd, Ni metal hydride, lead acid, alkaline, and thin-film batteries, all of which have significantly lower energy per mass. A comprehensive discussion of batteries is given in Chapter 6.

Table 10.3. Battery Types and Characteristics

Battery	Type	Cell Voltage (v)	Capacity (Wh/kg)	Discharge Current/Cell (mA)[a]
Alkaline[b]	Primary	1.50	336	NA
Lithium	Primary	2.80	260	NA
Lead Acid[b]	Secondary	2.10	252	200–5000
NiCd[b]	Secondary	1.35	244	10–1200
Ni metal hydride[b]	Secondary	1.35	278	120–3800
Lithium Thionyl Chloride[c]	Secondary	3.60	700	4–400
Thin film[d]	Secondary	3.80	100	1400–1700

[a]Typical discharge currents achievable. Values are dependent on size and operating temperature of battery.
[b]D. Linden, ed., *Handbook of Batteries*, 2nd ed. (N.Y.: McGraw Hill, 1995).
[c]Lithium Thionyl Chloride 3.6-V Batteries Technical Information, Tadiran, Ltd., Los Gatos, CA, June 1993.
[d]Bell Core polymeric mesh battery. (See Chapter 6.)

10.3.2.6 Communications

A large number of integrated circuits and circuit designs have been driven by the explosion in personal communication systems, such as cordless and cellular phones, handheld roaming inventory units, RF identification tags, and wireless LANs (local area networks). Many devices use digital methods of communication, and many commercially available chips and circuitry are driven by these applications. Some are listed in Table 10.4, together with derived communications requirements for the sensor master and ground transceiver. The reader is referred to a more detailed review and survey of spread-spectrum devices by Schweber.[27]

The user must be aware of potential problems in the design of a communication system. These problems include the effect of multipath signal channels due to reflections, Doppler frequency shifts, latency, bit-error rates, synchronization time, data-packet format, security, the pseudorandom noise (PN) code pattern to identify users, the modulation method used for spread-spectrum devices that define the "channel," the spectral efficiency of sending data per unit RF bandwidth, and finally, power consumption.

Elaborating further:

- Multipath reflections will often degrade the signal to noise at the receiver.
- Doppler shifts could reduce the coherency of the transmitted signals and cause a lowering of the signal to noise.
- Latency is the time taken to send and receive information in a propagated signal.
- The bit-error rates determine the required signal-to-noise ratio (S/N ratio) necessary at the receiver for each modulation method used. Often a bit-error rate of 10^{-6} is thought to be adequate for data, but for controls and commands a lower bit-error rate such as 10^{-8} is necessary. As one attempts to reduce transmitted power to conserve battery power for a mobile application, additional error correction may be necessary for commands and controls to achieve the necessary bit-error rate.
- Packet size is determined by the data content and the networking overhead information necessary to send and receive data.

Table 10.4. Derived Communication Requirements and Representative Implementations

Attribute	Sensor/ Master Req.	Master/ Master Req.	Master/ Ground Req.	Rf Serial Implementation	Rf Ethernet	PRISM DSS PC Wireless LAN
Peak data rate (Mbyte/s)	0.020	1[a]	10	0.0115 (UART limit)	0.3	0.1-0.2
IEEE standard	NA	NA	NA	RS-232	NA	802.11
Modulation	NA	NA	NA	NA	GFSK	QPSK, BPSK, or GFSK
Range indoor/outdoor (m)	10 indoor	100 outdoor	10^5 outdoor	90/900	161//910	120/1130
Rf power (W)	0.010	0.010	100	0.010	0.05	0.063
Antennas/gain	1	1	1	1-6	1-6	1
Bit-error rate	$<10^{-6}$	$<10^{-5}$	$<10^{-4}$	$<10^{-6}$	NA	NA
Data carrier frequency	NA	NA	<10 GHz	2401–2482	2401–2482	2401–2482
Channel access	NA	NA	NA	FHSS-CSMA or TDMA	CSMA/CA	CSMA or TDMA
FCC license requirement	NA	NA	NA	none (FCC 15.247)	none	none
No. of channels	17	30	1	82	15	82
All weather	yes	yes	yes	yes	yes	no
Vendor	NA	NA	NA	Digital Wireless	BreezeCom	Harris Semiconductor

[a]Assumes 10 submasters.

- Synchronization time is the time necessary for the receiver to synchronize its frequency-hopping pattern to the transmitter.
- The data-packet format that must be used includes all the data to synchronize, address, and quantify data length, and correct errors of the packet.
- Security may be necessary to prevent tampering with the packet or commanding of the system.
- The PN codes determine a predetermined frequency-hopping pattern for a given channel.
- The spectral density is a measure of how effectively a communication system is able to use its allocated frequency band.
- Power consumption is important as a parameter since it affects battery sizing.

Spread spectrum, in general, is a method by which a modulated carrier waveform is spread once by an intermediate frequency and a second time by a means independent of the information. For the direct-sequence spread spectrum (DSSS), a sinusoidal waveform with a frequency corresponding to the intermediate frequency, the ω_{if}, is modulated or multiplied by using a phase shift key (PSK) with an amplitude of +1 or −1 at a frequency corresponding to the digital baseband frequency, f_b. This baseband waveform consists of the binary sequence of information bits that will be transmitted. Lastly, the resultant signal is modulated once more by a spreading signal

function or PN signal, which has a modulation frequency, f_c. The final product of modulated signals is then up-converted to the carrier frequency. A number of simultaneous users are assumed to be broadcasting. At the receiver, the signal consists of the sum of all direct-sequence modulated signals plus additive white Gaussian noise and interference terms. The signal is demodulated, using the same PN sequence, with the result that only the desired modulated waveform remains. All other waveforms are spread over a much higher bandwidth. The despread signal is then PSK-demodulated to form the desired baseband signal, which contains the information that was transmitted in the original bit sequence. The probability of error in the received signal is a function of the number of users, the chipping rate (or the intermediate channel-hopping rate), and the bit rate. For code-division multiple access (CDMA), each user is provided with an individual PN code. If the codes are not correlated, then all independent users can transmit at the same time in the same bandwidth. The despreading in the receivers ensures that only the data sequence with the corresponding PN code is regenerated. CDMA systems can suffer from a near-far interference problem in which a near transmitter will mask the signal from a far transmitter. Adaptive power schemes have been proposed to solve this problem. The synchronization of a DSSS system is roughly equal to a multiple of the chipping period, $t = 1/f_c$, neglecting the additional time to perform the fine synchronization better than one chip period.

Spread-spectrum devices offer improved interference rejection, code-division multiple access, graceful degradation of performance as the number of users are increased, and lower implementation cost.[19] Commonly employed modulation schemes for spread-spectrum include, DSSS including CDMA, slow and fast frequency hopping (SFH or FFH), and carrier-sense multiple access (CSMA).[19]

For the SFH-SS and the FFH-SS, the binary PN-code generator causes the frequency synthesizer to hop from one of the many possible frequency bands selected by the generator. The RF signal is spread in a random fashion over the many available frequency channels. If the channel-hopping rate is slow compared to the bit rate, the system is referred to as SFH-SS. If the channel-hopping frequency is fast compared to the bit rate, the system is referred to as an FFH-SS. For FFH systems the probability of error is the ratio of the number of interferers with power greater than the carrier power divided by the number of channels available. As this number is often too high, forward error correction is used to reduce the probability of error to acceptable levels of 10^{-3} to 10^{-8}. For the purposes of synchronization, the FFH receiver can wait at a fixed-channel frequency and then advance in synchronism with the transmit FFH generator. This will correspond to about one hopping period at worst. Additional time must be allowed to fine synchronize, which may be a few multiples of the hopping period. In general, the FFH system will be able to synchronize faster than a DSSS system.

Error correction can give a decided advantage to the communication system by reducing the signal to noise needed at the receiver (transmitter) to achieve a given system probability of error but at the expense of transmitting additional bits and performing the additional computations necessary to correct or detect errors. Both functions result in some power penalty. With the properly designed code, a net gain in system performance is possible at the same transmit power.[19]

A block-error correction code is formed when a message or code word of k bits length is added to $(n\text{-}k)$ bits of redundant symbols. The total length is n bits for the code word that will be transmitted. The resultant code word is designated a (n,k) block code. The received code word is decoded by deciding that the most likely transmitted code word is closest in Hamming distance to the received code word. (The Hamming distance is the modulo-2 sum of the transmitted and received code words on a component-by-component level, with the assumption that the code words are represented as vectors.) Several codes are important. The (23,12) or Golay code is able

to correct for all patterns of three errors and offers an improvement in the bit-error rate by reducing it by more than 2 orders of magnitude at an energy of bit-to-noise-density ratio in slight excess of 8 dB. The Hamming (7,4) code can correct a single error with moderate improvements with an energy of bit-to-noise-density ratio of 8 dB. Comparison with other codes has been discussed by Feher.[28]

The allowed FCC bands for the carrier frequencies, the Instrumentation, Scientific, and Medical (ISM) RF bands, are located at 902-928 MHz, the 2.402-2.4835 GHz, and the 5.725-5.850 GHz. No licensing is required if certain restrictions are followed. A large number of devices for the two lower bands are available, driven by the growing widespread use of cellular phone technologies.

One of the most important standards for the implementation of LANs refers to the devices that follow the IEEE 802.11 standard for the 2.4-GHz band:

- Up to 1 W of power is allowed in the antenna.
- Data packets are restricted to 2048 bytes.
- The PN code length is 11 bits.
- Maximum data rates can be 1 Mbit/s for FHSS (frequency-hopping spread spectrum).
- The PN codes are used to define a frequency-hopping pattern. For FHSS both the transmitter and the receiver must periodically switch to a new carrier frequency.
- For the 2.4 GHz band, the hop rate must be at least 2.5 hops/s over the 79 sub-bands of 1-MHz-wide channels. This slow hopping rate should ensure complete transmission of a data packet before the next hop occurs.
- For the DSSS, the chipping rate or channel-hopping rate can be as high as 11 Mchips/s with 11 designated frequency channels, each with a 22-MHz bandwidth. The chipping rate is faster than the data rate, enabling processing gain.
- Maximum data rates for the DSSS can be 2 Mbits/s.

10.3.3 The Aerospace Launch Vehicle MPS System: Trade-Offs in Architecture, Requirements, and Design

The design of an MPS system is not always straightforward because of a variety of factors, including the availability of development tools, schedule, and development goals, and the availability of reliable chips, such as, sensors, processors, communication chips, and software. A designer of an MPS system rarely develops all the sensors, processors, software, networking protocols, power supplies, and communication chip sets. Instead, those subsystems for development and those for purchase will have to be adroitly selected. When funds are constrained, selecting COTS components would seem to minimize costs; however, this can be deceptive because consequent software development could be costly. Many components that are offered with software drivers, for example, will be suited only to personal computers, namely, PCs with a Windows® 95 operating system. Access to the source codes is often not allowed, given the competition of the commercial marketplace. Software availability or development cost for the driver software will be a major selection criterion for selecting COTS components in a plug-and-play environment.

A top-level design of a full-up networked MPS system was carried out for the full-up launch-vehicle application and is presented here together with critical issues that the designer would face. Based on the sensor survey, many MEMS accelerometers and pressure transducers would be suitable for the launch-vehicle application. For measurement of acoustic levels, small compact microphones are available in non-MEMS form. Two groups have developed MEMS microphones that may be suitable.[29] Strain gauges have been traditionally fabricated from resistive metallization on deformable thin, polymeric substrates that are readily bonded to a surface undergoing strain

deformations. Numerous temperature sensors are also available such as thermocouples and platinum resistance devices. For temperature and strain, the sensor must be physically isolated from the MPS node to prevent erroneous readings caused by effects of the thermal mass or the elastic modulus of the node, which includes the processors, batteries, transceivers, external case, etc. Many sensors include some form of signal conditioning; calibration of the sensor and signal conditioner is needed. Some sensors provide for a built-in functional test; detailed calibration must still be performed by the user.

A hierarchical networking architecture was selected (Fig. 10.2) and sensors were assigned to numerous engine compartments of the launch vehicle. An average of 50 sensor locations are assigned to each compartment for a total complement of 10 compartments. The compartment metal walls are not conducive to RF transmission, and a port or gateway is necessary to communicate between compartments. This may be accomplished using a small wall penetration, for example, with an antenna on one side and the processor on the other. The distance within a compartment is quite small, approximately 10 ft across, often with no direct line of sight from node to node. In each compartment a local network could be configured with one or more masters that would enable communication to other masters outside. These masters can then communicate and direct data or commands upward or downward in the hierarchy. This scheme allows an advantageous reuse of the RF components and spectra inside each compartment.

Data sent up the hierarchy through the masters will then reach a transmitter capable of communicating to a ground unit. The transmitter on the ground will have a high-gain antenna to receive the RF signals with a processor to perform network control, collect data, unpack the packets, archive data, and perform data analysis. There will be an asymmetry in the upward data flow

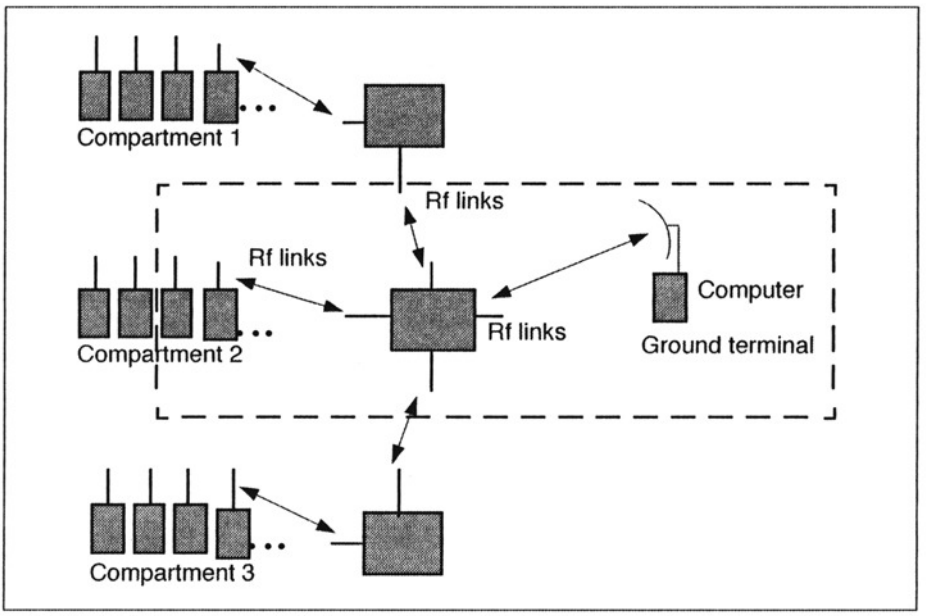

Fig. 10.2. Schematic architecture for the data flow of an MPS consisting of a large number of sensor nodes, at least one master node for each compartment, and a single ground node. The full system may consist of up to 500 sensor nodes organized in this hierarchical structure. The "command" communication network is not shown. The dashed lines outline the portion of the full system that was selected for a demonstration; it consists of two sensor nodes, one master node, and one ground node.

from the sensor nodes, as discussed earlier, versus the downward flow of data and commands to the sensor nodes.

An alternate scheme of direct communication between each sensor node and a ground terminal was rejected for the following reasons. Each sensor node must have access to an outer wall for an antenna to link with the ground, requiring too many compartment wall penetrations and a more complex installation. The transmitter power and electrical power for each terminal must be high enough to complete the link to the ground and would require either an adaptive power transmission strategy using vehicle location to enable a small physical size for each sensor node or a large battery size.

The network is designed for several modes of operation: installation, test, launch standby, operation, and sleep. The system will be installed at the factory because of the large number of nodes (up to 500) that must be employed. During the installation mode, the network system is installed and integrated. Once the master nodes are in place, individual links can be tested. A separate installation master is preferred when installing a single sensor node. The test mode is invoked to verify that the installed system is capable of the mission function. Prior to the launch, the system will be placed in a sleep mode to conserve power, for which there are several strategies. For example, with a single low-frequency watchdog timer on each processor, the sensor node could wake periodically, perform a self-test, move into a receive mode, wait for commands from the master, transmit its status, and return to sleep. Alternatively, the ground terminal could request a self-check until the masters awaken to test their sensor nodes and return them to sleep. Total active data-logging time is 10 min, which is the flight duration for a Titan IV. Tens of minutes before launch, the system will be placed in a standby mode. Since launch countdowns are often interrupted, the system must decide whether to stand down and store power, and it must be able to transition from one mode to another. Precautions may be necessary to avoid inadvertent mode transitions or tampering with the system configuration.

The functions of the sensor microcontroller are to convert analog signals to digital levels, sample all sensors at the requisite sample rate, form a data packet that is time tagged, send it to the appropriate network node, receive and execute commands from the master, and place itself in the appropriate network mode. It may also perform thresholding or data analysis as a means to reduce data. In addition, it must inform the master periodically of its health status, especially during active data-gathering if no data are sent because of thresholding. The raw data from each compartment is 1/10 of the total, or 10 Mbits/s. This rate is within a factor of 3–5 of present Ethernet data rates. For inexpensive hardware, wireless LAN data rates are at the 1–2 Mbits/s rate and will soon be increased to 10 Mbits/s.[30] While a combination of thresholding, data compression, and peak off-loading could reduce net data being transmitted, peak off-loading may only be useful for a normal successful launch. The one caveat of peak off-loading is that during an unsuccessful launch, the system may have programmed assumptions about the integrity of the system throughout its entire mission life, which may become invalidated and lead to loss of critical data describing the failure.

Certain high frequencies at low power that may be used for the small range within the launch vehicle cannot be transmitted at long range in the atmosphere. For transmission from space to ground stations at the typically long-slant ranges in excess of 100 km, the atmosphere is transparent only below 15 GHz.[31] Since the data rates scale with carrier frequencies, there is an upper limit on total peak bandwidth for data transmission. But for the 2.4-GHz ISM band with modest data compression, this is not expected to be a major problem.

Selection of processor hardware is often driven by the availability of supporting software, chips, or dies that meet environmental specs and processing needs, and development tools for

software and diagnostics that can work with brass-board hardware to solve implementation problems, such as, timing, connections, and proper instruction sets.

Once software and data storage is sized based on the algorithms and protocols required, the processing speed can be approximated from how frequently the cycle of data taking, data storage, packet formation, and communications occurs along with an estimate of the networking servicing overhead. For this project, a 32-bit processor of the Intel-486 class was selected as adequate for the sizing of the processors used for the sensors and master nodes. Many equivalent processors/boards able to support the necessary digitizing rates are listed in Appendixes 10.B and 10.C. This demonstration system stressed function over form; thus a palmtop PC for which drivers are available for the PCMCIA cards was deemed acceptable.

Several networking issues identified included latency of networking services such as time distribution or synchronization, fault tolerance, command and control, and differing protocols and data rates for sensor data and network commands. At high bandwidths, error correction and scaling to support high data rates are additional concerns.

For communications, the advantage of frequency reuse is inherent in the hierarchical architecture defined by the compartments of the vehicle (which form natural cells) and the metal compartment walls. This allows implementation of identical architecture from cell to cell. Moreover, if compartments are indeed isolated from the exterior, the identical frequencies may be reused for the master-to-master communications. Within a cell, a simple token passing scheme of the sensors by the appropriate master, a form of time division multiple access (TDMA), could be used to meet required communication rates. This may be easier to implement using a single transceiver on each sensor node and a single transceiver on the master. Multiple transceivers may also be used on the master to increase the total data rate to the master, but at the expense of greater hardware complexity and power.

The explosion of personal communication devices such as cellphones and pagers during the 1990s was realized using digital techniques. Digital communication has the following advantages.

- Allows improved RF spectral utilization or capacity
- Enables digital data compression methods
- Reduces overhead for signaling over analog methods
- Enables a robust source and channel coding methods
- Improves performance during interference due to cochannel and adjacent channel interference
- Allows flexible bandwidth allocations to meet demand
- Expands the services over analog systems (such as, data services, encryption, authentication)
- Improves access and hand-off control.[19]

In the near future, a large number of spread-spectrum devices will become available with the necessary bandwidth. In 1996, many fast serial RS-232 digital RF transceivers were available. For the purpose of real-time control, these serial implementations could be chosen despite their slower data rate. For the purposes of a demonstration, the current data rates are satisfactory but would need to be increased for a larger, high-data-rate system.

Power for the entire system will probably come from stored battery energy. The necessity for power management when using battery power is demonstrated by the following example to calculate battery capacity. A PIC 17C756 microcontroller and a Harris PRISM chip set were used, and calculations for a sensor node and a master node were performed. The sensor node for this exercise has three analog-device accelerometers, a single PRISM transceiver, and a single PIC microcontroller. The master node has one microcontroller and two transceivers. Calculations for power consumption are done for the network in the sleep mode and the active mode. The sleep

mode duration is assumed to be 60 days, and the active mode, 10 min. During the sleep mode the sensor node must occasionally transition the microcontroller from sleep to active mode to turn on the transceiver for a period of 5 s every 30 min. During this brief "on" mode, the node must go through a warm-up/stabilization period and discern whether the master node is attempting to command it to remain awake. If no wake-up call is received, the transceiver is turned off, and the microcontroller goes back to sleep until the next cycle. The power of each device is summarized in Table 10.5.

The sensor and master nodes sleep-mode consumes the bulk of the power because of the "on" status of the microcontroller and transceiver. If the on/off duty cycle time can be reduced further, a more favorable sleep-to-active mode power utilization is possible. For the master node during sleep-mode, the transceiver outside the compartment must listen and react to messages destined for each compartment. The master then transmits the message to the sensors assigned to it. To simplify matters, we assume that the transceivers are on for 5 s and cycle through this routine once every 30 min. Obviously we neglect the energy to perform the transmit portion of the wake-up call, which will occur periodically over a maximum time span of approximately 30 min. During the active mode the master node has the transmitter and microcontroller "on." For this design, greater than 95% of the total stored energy is used during the network's sleep mode. If we use lithium thionyl chloride batteries, the weight of the batteries for the sensor and master nodes will be 3.8 g and 6.6 g, respectively, not allowing for any margin or battery package. This calculation has not properly accounted for the additional time that the controller and transceiver must be on to precede the event to be monitored by the system. The system will be awakened to the nearest period preceding the time of the active event. Prior to the 10-min active period, the system could be awakened as early as 30 min before the actual event, and the maximum time of the active mode will stretch to 40 min.

For many systems requiring a significant period of sleep time or shelf storage time, the designer must implement a low-duty-cycle sleep time to prevent sleep power requirements from dominating the battery sizing. Other strategies to reduce power loads include placing the transceivers temporarily into other energy conservation modes as allowed by the chip designers, using low current leakage, miniature mechanical or MEMS relays to turn power on or off, capacitive sensors, and additional techniques available to the designer of a μCluster as discussed in Subsec. 10.6.4.4.

Table 10.5. Device Power Consumption for Sensor and Master Nodes in Sleep and Active Modes

Power	Sensor Node Sleep	Sensor Node Active	Master Node Sleep	Master Node Active
Accelerometers (mW)	0	150	NA	NA
Microcontroller (mW)	0.055	150	0.055	150
Transceiver (mW)	0	460	0	920
Sleep-mode duty cycle (on/off in s)	5/1795	NA	5/1795	NA
Subtotal (W-s)	9.1×10^3	4.6×10^2	1.6×10^4	6.4×10^2

10.4 The Plug-and-Play COTS Approach

A test bed was constructed using COTS components for the networked MPS system. The approach was to demonstrate function rather than meet form and fit functions. Available components were chosen primarily for rapid implementation rather than for the comprehensive requirements for the full-up launch-vehicle networked MPD system. Any shortcomings in meeting full-system requirements are noted.

Two sensor nodes, a single master node, and a single ground-terminal node were designed and integrated. See Fig. 10.3. (The relationship of the selected demonstration to the full system is shown in Fig. 10.2.) For the sensor node, a set of three accelerometers for three-axis sensing and a single pressure sensor were chosen as representative of high and low data-rate sensors. For the microprocessor, a palm-sized 486PC and an ADC PCMCIA card were selected. The communication subsystem was implemented using an RS-232-based spread-spectrum transceiver, one unit per sensor node.

The master node used a 486PC for its processor and identical transceivers, one for each sensor node and another for the communications to the ground terminal, for a total of three transceivers. The ground terminal used a single transceiver and a laptop using Labview, a commercial instrumentation software with a graphical user interface. The assembled system is shown in Fig. 10.4 and is described in the following section.

10.4.1 Selected Sensors

Three different accelerometer models were chosen for the COTS demonstration.

- Silicon Design, Issaquah, Washington: 1210-50-J single-axis and 2412 three-axis
- EG&G IC Sensors, Milpitas, California: 3255-050 and 3255-500 single-axis
- Motorola, Phoenix, Arizona: MMAS40G10D single-axis

The first two sensors had adequate bandwidths of either 1.6 kHz or 2.0 kHz, but the third had a reduced 400-Hz bandwidth, inadequate for the launch vehicle application. It was selected because it was one of the cheapest accelerometers available at the time, but many MEMS accelerometers of suitable bandwidth and range for the launch-vehicle application are now available.

The Analog Devices 5-g accelerometers were selected for further calibration studies. In the dc mode, calibration can be accomplished by orienting the sensors in three directions to the Earth's

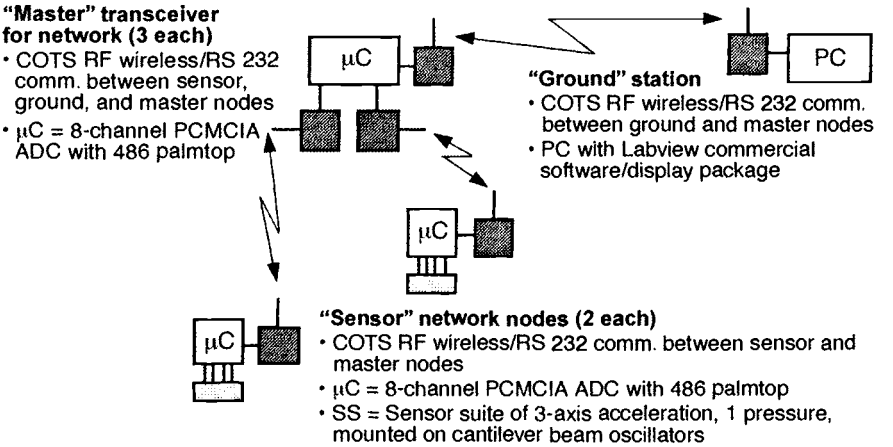

Fig. 10.3. Schematic of the functional networked MPS system. The four nodes depicted are two sensor nodes, a master node, and a ground terminal.

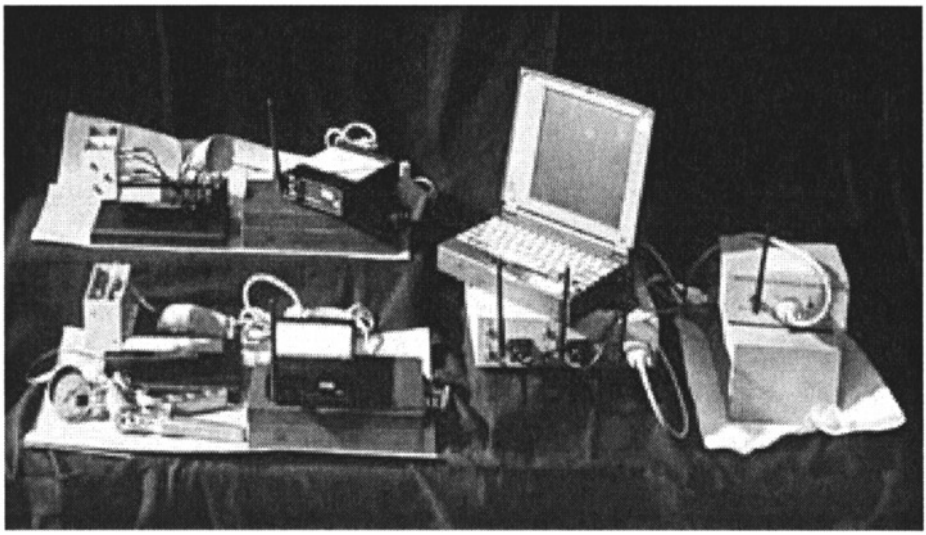

Fig. 10.4. COTS implementation of a partial MPS system (as shown in Fig. 10.2). The two sensor nodes are located to the left above one another. To their right is a single master consisting of three transceivers and an open palmtop computer. The ground terminal, consisting of a single transceiver, is shown to the right of the master. The laptop was not available at the time of the photo.

gravitational field, +1 (with), 0 (perpendicular), and −1 g (against). These sensors have a built-in amplifier to enable ac or dc coupling, variable gain, and zero-offset. The accelerometers are very linear over their range, and the slope responses can be reproduced to within 5% of one another.

10.4.2 Processor and ADC

The processor hardware includes three 75-MHz, 486 palmtop computers (model iLuFA 350 from Chaplet, Sunnyvale, California) for the sensor and master nodes. The palmtops support PCMCIA plug-ins, which include a 100-kilosamples-per-second A/D converter (model DAQ Card-1200 from National Instruments, Austin, Texas) used in the sensor node and additional serial ports (model MP540301 dual high-speed serial card from Mobile Planet) used in the master node. The palmtop computers were selected for their small physical profile and the readily available PCMCIA plug-ins and drivers for DOS or Windows® 95. The ground node is simulated using a Pentium, 133-MHz laptop PC (Hitachi model E-133TC).

The ground terminal was developed using a Labview software package,* a commercial, graphics-based software/hardware interface to accept the time-tagged data packets and to display the resultant waveforms in real time for a demonstration. The ground terminal displays the digital output of the pressure sensors and an operator-selectable time duration for the display of the 3-axis accelerometer data of amplitude versus time. Data from both sensor nodes are displayed simultaneously to present visual feedback to the operator.

10.4.3 Communications

Three pairs of wireless, 2.4-GHz RF spread-spectrum, RS-232 transceivers were selected for serial communication between the sensor and master, and for the master to ground links. The transceiver (Digital Wireless, model WIT 2400) is implemented on a printed circuit board with

*Labview software is available from National Instruments.

2.4 × 3.0-in. dimensions. Additional space is needed for an antenna and a small circuit to convert RS-232 serial voltage levels to TTL voltage levels. A robust sensor-network communications protocol was designed that emphasizes flexibility, simplicity, and bandwidth conservation. An amplitude thresholding concept was used to reduce the data being reported by the system. Since data below a predetermined threshold are not reported, the data packet protocol employs time stamping for each reported sensor amplitude. One novel feature of the protocol is that it supports a wide variety of error correction techniques that can be selected by the network user to balance data integrity with bandwidth consumption. The protocol, in its current form, will support fewer than 10 sensors.

10.4.4 Assembly and Testing

All major components of the software were developed in parallel to hasten development time, including the complete network stack, the software libraries for the data acquisition hardware, and the application layers for the multiparameter sensor demonstration. The "spiral model" of software development was selected for its characteristic rapid, repeated cycle of incremental design, implementation, test, and integration. This process ensures that at each stage in the development cycle, successive versions of the system are integrated, bug-free, and meet performance requirements.

High-speed serial drivers were developed, which are capable of providing the maximum performance with a PC-compatible architecture and use the maximum transfer rates provided by the spread-spectrum RF transceivers. Initial timing studies of the data acquisition rates were performed on the hardware selected for the prototype. The goal to acquire 2,000 samples per second for each axis of the three-axis accelerometers was easily met. A total acquisition rate of 12,000 samples per second has been achieved, which is twice that required for the prototype demonstration. This limitation, consistent with model prediction, is dominated by the fundamental transmission rate of the RS232 hardware and the UART hardware (both are specified at 115 kbits/s) and not by the data acquisition hardware speed or the software execution speed. The observed data rate is adequate for many space applications using a small number of sensor nodes. Larger numbers of sensor nodes can also be supported, but the master-to-master link must support a rate slightly larger than the sum of sensor-to-master data rates. For the master-to-master link, the present implementation of RS-232 would be inadequate. Faster transceivers at 2 Mbits/s using other protocols such as 10 Based T Ethernet or the IEEE 802.11 standard could be used to improve throughput either at the sensor-to-master or master-to-master links. For the full-up system using data compression techniques, load averaging methods, or upgrading to a faster IEEE 802.11 device, the master-to-master link requirements would be satisfied.

10.4.5 Second Generation Multiparameter Sensor System

The development of a second-generation MPS system sensor concept[32] is under way to achieve a miniaturized sensor node using the PIC 17C756 microcontroller and an RF-communication, PCMCIA card that uses the IEEE 802.11 standard for the 2.4 GHz band. The master node consists of identical RF-communications cards, a laptop computer, and Labview software that displays data and provides rudimentary system commanding, system-mode control, and data archiving. The goal is to achieve the first milestone of developing compact hardware and corresponding software capable of high-speed (1–2 Mbits/s) communications that could be used in applications similar to that of the launch vehicle previously discussed. The architecture of the sensor nodes is organized into custom sensor and processor boards, a networkable RF-PCMCIA card from Harris, and a custom battery pack. The sensor board includes 3-axes accelerometers, pressure transducer, humidity sensor, and temperature sensor, all with appropriate signal conditioning. The processor

board includes the PIC microcontroller, 4 Mbytes of memory, an ACTEL-programmable gate array to interface the processor to the memory, and the RF card. The system modal diagram supports the following modes: sensor-node installation, calibration and status check, data acquisition and temporary data storage, power savings (sleep), and data reporting/command response to the master. The first milestone consists of the completed sensor node sending data to the master. Network self-configuration and other network controls will be implemented as a second milestone, with field testing implemented as the third milestone.

Development is 80–90% complete for the first milestone. Nearly all software modules have been designed, implemented, and tested piecewise, except for the RF-communications module. The microcontroller and software for data acquisition have been tested, and a maximum of 12 Ksamples/s cumulative measurement rate is projected using 6 ADC channels. However, additional time allocations for RF transmission and overhead were not included in this estimate. The mechanical design of the enclosure and edge connectors were completed and will undergo shaker testing to validate the robustness of the design. The custom sensor board has been designed and is undergoing testing. Complete circuit designs are awaiting the details of the RF-programmable gate array and are estimated to be 90% complete. Once the design is completed, breadboard hardware will be assembled to integrate and test the entire design, with anticipated completion in early 1999. Final sensor nodes will be available shortly thereafter.

10.4.6 Summary of the Aerospace COTS Development

A high-data-rate, MEMS-based instrumentation system concept to demonstrate function was designed, based on the wireless, high spatial-density-measurement requirements for a launch vehicle environmental monitoring application. Commercially available components, including sensors, processors, A/D converters, and wireless RF transceivers, were selected for the development of a demonstration based on a subset of the full-sensor network. The demonstration required the development of protocol design and implementation, including network stack, software libraries, timing tests, and network throughput. Scaling issues to the full-system performance were identified. Many of the concepts and sensor hardware could be easily reused for a microsystem of small form factors.

A second-generation sensor-node development was initiated as a direct design of an MPS system. Its emphasis is on high-speed data acquisition and data reporting similar to the launch-vehicle application. The sensors include commercially available accelerometers, temperature, pressure, and humidity sensors. The processor is a PIC 17C756 microcontroller and a networkable RF transceiver. About 80–90% of the hardware and software design is completed. Piecewise testing/simulation of hardware and software was completed, but final integration and test will occur when the software module is completed. The RF software module will lead completion of the final design late in early 1999.

10.5 Wireless Integrated Network Sensors

A concept developed at the University of California, Los Angeles, to monitor and control a system capable of networking, signal-processing, sensing, and decision-making at low power with RF communications shows great promise for a variety of applications.[33] These applications include transportation, manufacturing, health care, environmental, and safety and security monitoring. The system is referred to as the Wireless Integrated Network Sensors (WINS). Size of a sensor node board is approximately 1×2 in.

The architecture of the sensor node includes components for sensors, an ADC, a spectrum analyzer with a set of analog filters on the input, memory buffer, a microcontroller, and RF transceiver. The WINS system, a collection of sensor nodes with a gateway to a more conventional

network, is capable of acting as a distributed sensor network. The sensor suite consists of a dual thermopile and horizontally and vertically sensing accelerometers. Each thermopile consists of 32 elements of a bismuth-antimony junction capable of 1.8 nW/(Hz)$^{1/2}$ sensitivities. The accelerometers have sensitivities near 2.4 mg for frequencies near 11 Hz. For a band centered at 5 Hz, the sensitivity is 10-7 g/(Hz)$^{1/2}$. The spectrum analyzer and sensors are on continuously. The spectrum analyzer output triggers a wake call to the microcontroller that determines the next course of action of either additional processing or notification of a user or neighboring node. This design is tailored toward detection of vibrations, especially those caused by rotating machinery or repetitive phenomena and temporal changes in infrared (IR) signatures detectable with poor spatial resolution, presumably large objects in the field.

Power utilization is a concern in the design of the WINS system. Low power of less than 30 μA is needed with peak power less than 3 mW; compact Li-coin cell batteries are used. The sensor node RF range is limited by the low-power transmitter of 1–3 mW and by the power and sensitivity to noise of the receiver. To reduce receiver noise, a high Q, LC circuit design was implemented for the voltage controlled oscillator (VCO) in the receiver. A low-power mixer was also designed, using 0.8 HPCMOS (high-performance complementary metal oxide semiconductor). The mixer modulates the carrier frequency at 900 MHz. Power dissipation for the receiver oscillator is 300 μW at 500 MHz and for the mixer, 70 μW at 3 V. These are some of the lowest power CMOS RF oscillator and mixer reported. Overall system communication power can be optimized by relaying information in multiple hops, compared with the use of a single hop with a higher power transmitter in a multipath RF signal propagation environment. A second strategy to reduce power is to increase the delay time for event recognition, which allows for reduced power in processing and computation. This is ideally matched to low-bandwidth sensors of less than 10 kHz.

In summary, a very compact, low-power, low-cost data reporting system was built with the potential for applications in environmental monitoring, safety, security, manufacturing, biomedicine, and condition-based maintenance.

10.6 Design of a Microinstrumentation Cluster

The University of Michigan Microinstrumentation Cluster, or μCluster,[34] takes a different approach to microsystem design. The μCluster is a multiparameter sensing system that supports a variety of MEMS sensors within each sensing node of a macrosystem. Work on the μCluster project focused on the development of individual microsensors and the definition of a generic microsystem architecture with flexibility to meet the requirements of many different sensing applications. Throughout the development, a number of interesting trade-offs have been analyzed. Since many of these will be common to any similar microsystem design, they are discussed in this section.

10.6.1 μCluster Requirements

When designing a microsystem from the ground up, the first step is to determine the goals of the intended system. For the μCluster, the goals were the following.

- Create a generic microsystem that would support a wide variety of applications simply by changing the system sensors (and possibly modifying the control software). The intended applications range from distributed environmental monitoring to industrial process control.
- Provide a standard design for the individual sensor nodes (microsystems) that could be used within each macrosystem.
- Select a specific application for which a prototype system could be designed, in order to establish specific design requirements of the μCluster. Environmental monitoring was selected.

- Create a system capable of monitoring its environment and its position within that environment while operating at micropower levels from its own battery supply, communicating to a host system via a wireless link, and maintaining a small physical size.
- Develop capability for the microsystem to enhance sensor performance and functionality with system-level features, respond to event-triggered interrupts, and utilize in-module digital data compensation.

To accomplish these goals, the microsystem must have the following features.

- It must utilize some sort of internal sensor bus to which (almost) any sensor can be attached provided it has the proper interface hardware. This sensor bus makes the microsystem architecture independent of any specific sensor or sensor technology and makes it easy to add or remove sensors from the system.
- To operate at micropower levels, the μCluster uses only low-power components (i.e., capacitive sensors) and employs a power-management scheme involving both hardware and intelligent control.
- Wireless communication requires the microsystem to have an on-board transmitter for data output and a standard output format so that the data can be received remotely.
- Minimizing the physical size of the microsystem requires limiting the number and size of components (including batteries) and identifying an appropriate packaging technology.
- Some built-in intelligent control is needed to allow in-module decision-making and data-manipulation.

Thus, the μCluster must bring together low-power electronics, state-of-the-art microsensors (and perhaps microactuators and microinstruments), and wireless communication to form a standalone intelligent microsystem capable of delivering processed sensor data/information to a remote host as part of a network of similar microsystems.

10.6.2 Generic Microsystem Architecture

Once the overall system features are identified, a block diagram of the microsystem can be constructed. From a macro-system view, it is assumed that there will be a single host system that receives the data from the individual microsystems. In some applications there may be many microsystems for each host; while in others there may be only one. The μClusters would connect to the host through a networking scheme similar to that discussed in Sec. 10.3. In defining the microsystem architecture, a great advantage is to provide a generic structure that can support a variety of sensing applications. A generic open architecture allows individual aspects of the microsystem to be altered without affecting the entire system; for example, with generic open architecture, a system that measures temperature and humidity could be converted to a two-axis accelerometer simply by changing the sensors (and control software) but retaining all other system features. The alternative would be to design application-specific microsystems that have no common structure and require redesigning from the beginning each time a new application is to be supported. A generic open architecture also provides a set of standards for the individual components of the microsystem. Once in place, these standards simplify the design of both sensors and new microsystems by establishing a fixed protocol for communication between components.

The controller to provide intelligence and programmability will, in essence, be the heart of the microsystem and is a good starting point to define the system. Next, the generic microsystem modular approach to sensor population will allow each front-end sensor chip, which may contain a variety of sensors and actuators (addressable elements), to be considered as an individual module that can be replaced without altering the rest of the system. Each such sensing node must have all the necessary electronics for making measurements, converting data to a standardized output

format, and communicating this information to the microsystem controller. To accommodate multiple sensing nodes within the microsystem, a standard sensor-bus format (and related protocol) must be established to allow communication between the controller and the local network of sensor nodes. The internal sensor bus must be defined in a way that is generic and yet covers the needs of a variety of sensors. The sensor bus must allow for sensors to be removed, added, or exchanged without altering the bus itself. An appropriate sensor bus capable of these features is discussed in Subsec. 10.6.4.1. Ideally, the sensors could be added/exchanged without external modification of the system software (e.g., the sensor node would automatically upload its control/personality information to the microcontroller on system power-up).

A wireless communication link and some power-management features complete the system block diagram. Because of size and power limits, the wireless link will be an RF transmitter capable of transmitting an appropriate (e.g., amplitude-shift-keyed) output format. This format will also simplify the system by using the same protocol for both wireless and hardwired output connections. A variety of concerns regarding power management must be analyzed in order to provide a generic approach to this complex issue. This will be discussed in detail in Subsec. 10.6.4.4, but for now it can be assumed that power management is another block that interacts intimately with the controller. This is shown in the block diagram of Fig. 10.5, which illustrates the necessary building blocks for the generic microsystem and how they interact. The illustration also provides additional information as to how the individual sensor nodes can be viewed, either as a single block or as several interconnected blocks. The significance of this will be addressed in subsequent sections on sensors and packaging. Each microsystem building block is discussed individually in the following section. The trade-offs in choosing each component will be discussed as well as how these choices affect each other and the final microsystem definition.

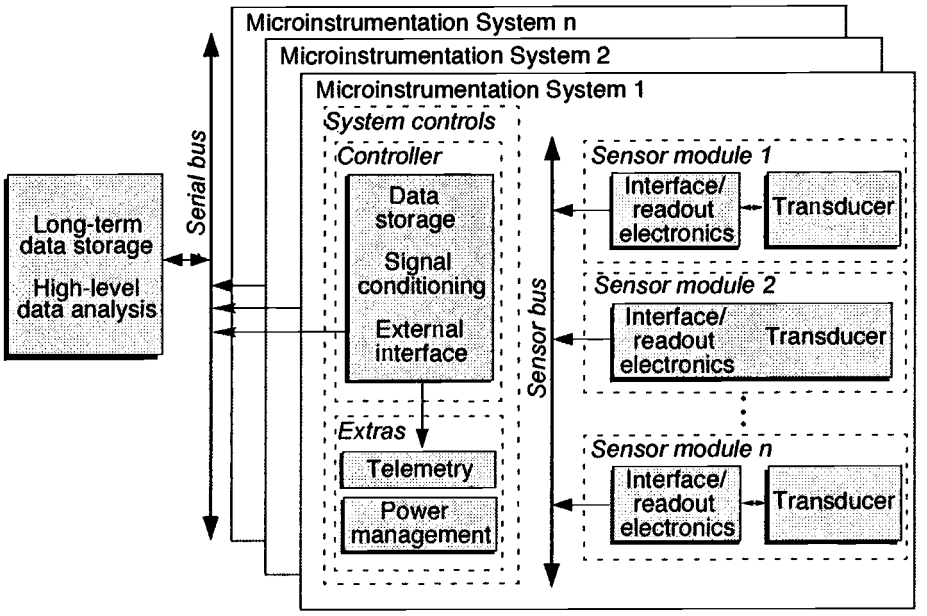

Fig. 10.5. System architecture block diagram for a generic microsystem. This architecture has been adopted by the University of Michigan Microinstrumentation Cluster, called the μCluster. This diagram shows the microsystem-level architecture as well as the position of each microsystem in the overall macrosystem that joins multiple microsystem sensor nodes to form a distributed sensing system.

10.6.3 Integrated Sensors and Microactuators

Highly integrated microsystems such as the μCluster depend on low-cost microprocessors and memory and on the ability to form the front-end transducers.[35,36] The first integrated silicon sensors emerged in the mid-1960s in the form of visible imagers. These devices required no process technology other than that used for integrated circuits, and the only packaging modification was use of a transparent window in the package lid. Visible imagers have been continually improved over the last 30 years and are now approaching the resolution of photographic film. Video cameras have replaced movie film with magnetic tape, and digital still cameras are now entering the mass market. By the early 1970s, the first selectively etched pressure sensors were reported,[37] but it was not until the early 1980s that high-volume products began to appear using micromachining (i.e., the precision etching of three-dimensional microstructures, usually in or on silicon). The first of these products were pressure sensors,[38] followed by accelerometers,[39] flowmeters,[40] and other devices. Most of these devices have been driven by automotive applications or by applications in health care. Monolithic gyros[41,42] are now in development, along with increasingly complex microinstruments. Of the different parameters to be measured, pressure, force, and acceleration have yielded well to transduction by silicon microstructures, and the high accuracy rate of these devices rival the capabilities of monolithic data converters. Near-inertial-grade accelerometers and gyros will likely emerge during the coming decade and, combined with the global positioning system (GPS), should come to be widely applied for precise position sensing, tracking, and navigation. Thermal devices have been readily integrated in silicon for monitoring temperature, and micromachined devices that utilize dielectric beams and diaphragms are creating a paradigm shift in IR imaging.[43,44] Magnetic devices have not yet made extensive use of micromachining, but magnetometers and Hall devices have been realized in silicon for many years. Chemical devices (e.g., for exhaust gas analysis, process control, and pollution monitoring) remain among the most needed of all sensors, and yet their problems are among the most complex. Nevertheless, approaches based on micromachining are among the most promising for these devices as well.

Ability to form microactuators on or in silicon added a new dimension to microsystems in the mid-'80s. Lateral comb resonators[45] have been widely employed in accelerometers,[46] tunable micromechanical filters,[47] and elsewhere. Microactuation is more difficult than microsensing, and many near-term microactuators will likely continue to be embedded devices used for self-testing sensors. Exceptions are found in projection displays based on micromirrors[48] and in microvalves.[49] Micromachined silicon-based fuel injectors have also been realized with some success.

10.6.3.1 Technology Options

In the fabrication of integrated sensors and microactuators, all of the technologies developed for integrated circuits are used. In addition, special technologies are employed to create microstructures (diaphragms, beams) for transducing the variables of interest. These special technologies are micromachining, wafer bonding, and electroforming. See Chapter 1 for more details of microfabrication methods and options.

10.6.3.1.1 Micromachining

As originally applied, the term "micromachining" referred to selective etching of the silicon wafer ("bulk micromachining"). Early efforts on beam-led integrated circuits* at Bell Telephone

*Beam-lead integrated circuits (electroplated lead-tabs that extend beyond the chip) were developed in the early 1960s at Bell Telephone Laboratories. They were a flip-chip technology compatible with hybrid thin-file passive components on ceramic. Widely used until the mid-1970s, beam leads are still used in some sensor and display approaches.

Laboratories led to the development of isotropic and anisotropic silicon etchants. Micromachining switched to the anisotropic etchants in the early 1970s to reduce undercutting, reduce agitation sensitivity, and allow the use of impurity-based etch-stops (Fig. 10.6). Silicon etchants such as ethylene diamine pyrocatechol (EDP) attack the <100> directions in silicon much faster than the <111> directions, and the existence of a highly doped (p++) boron layer in the silicon results in a rapid falloff of etch rate,[50] creating an etch-stop. Thus, a simple boron diffusion can be used to retain bulk silicon layers from 1.5 to 15 μm thick with no critical timing of the etch. Since the doping levels in p++ silicon are too high to permit electronic device fabrication, the etch-stop is sometimes used as a buried layer [Fig. 10.6(b)]. An alternative is to use an electrochemical etch-stop [Fig. 10.6(c)], which requires a bias distribution network on chip and more elaborate etching procedures, but is also coming to be widely used. Recently, there has been the increased use of devices in which front-side patterns oriented along the <100> lateral directions in silicon are undercut. These structures are more quickly formed than the back-etched structures and are more compatible with standard foundry process flows. Dry etching[51] is also being increasingly used both for shallow etches and for deep high-aspect-ratio devices. Aspect ratios exceeding 30:1 can be achieved.

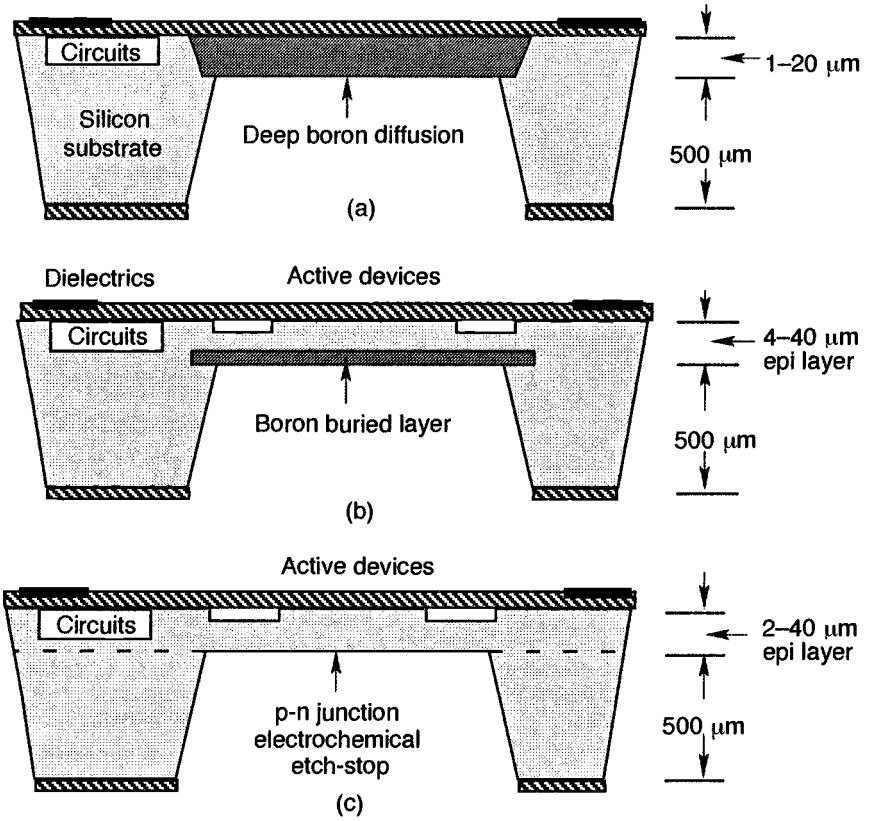

Fig. 10.6. Impurity-based etch-stops in bulk micromachining. Use of (a) simple boron diffusion, (b) diffused boron buried-layer, and (c) p-n junction epi-substrate etch-stops are illustrated.

10.6.3.1.2 Wafer-to-Wafer Bonding

In electrostatic (anodic) bonding, the silicon wafer is placed against a glass substrate and heated to a temperature of 400°C–500°C. The glass is chosen to closely match the thermal expansion coefficient of silicon, with Corning 7740 a common choice. From 400 to 1000 V are applied across the silicon-glass interface, which pulls the two materials into intimate contact and fuses the materials in a seal that is stronger than either of the materials separately. The advantages of these structures include relatively simple wafer alignment (the glass is transparent) and low parasitics. However, the glass is more difficult to cut than silicon, and the thermal expansion coefficient is not a perfect match to silicon, giving rise to temperature sensitivity. Where better temperature matching or on-chip circuitry is desirable, direct silicon-silicon fusion bonding is possible.[52] Two silicon wafers are cleaned, placed in contact, and heated to temperatures typically exceeding 1000°C. The materials bond to effectively form one piece of material. Where silicon-glass anodic bonds will form across surface steps of several hundred angstroms, silicon-silicon bonds require surfaces that are flat to within angstroms and very clean. The high annealing temperatures can also compromise some processes. Nevertheless, silicon-silicon bonding can create unique microstructures, and its use is increasing.

10.6.3.1.3 Electroforming Processes

A third approach to achieving three-dimensionality involves electroforming. An old technology used in the early days of integrated circuits, it has been recently rediscovered for integrated sensors. Using photoresist, or polyimide defined using dry etching, as a plating mold, it permits the batch formation of rather thick metal structures. In the widely publicized LIGA process,[53] X-ray lithography permits the formation of very thick structures (>1 mm) using electroplated nickel. Very high aspect ratios are possible in such devices at the cost of a synchrotron source. The process offers unique capabilities for devices that can be produced in no other way.

10.6.3.2 Device Options

Bulk micromachining has been discussed above for the formation of beams and diaphragms from the wafer bulk. Front-side bulk processes that undercut the microstructure [Fig. 10.7(b)] are especially compatible with foundry fabrication, typically require no modification of the process flow except for a final etch just prior to die separation, and are also becoming increasingly used. Surface micromachining[54] emerged in the mid-1980s as an alternative to bulk processes. In surface micromachining [Fig. 10.7(c)] a sacrificial layer (usually phosphosilicate glass [PSG]) is deposited on the wafer and patterned. The intended microstructure material (polysilicon or metal) is deposited over it and patterned so that it anchors to the wafer over the ends of the sacrificial material, which is subsequently removed to leave a beam, cantilever, or diaphragm. Such devices have been used for accelerometers,[46,52] for pressure sensors (using seals provided by CVD dielectrics),[55] and for other microstructures. Control of stress in the deposited layer is an important challenge with polysilicon high-temperature (>1000°C) anneals generally required. Stiction[56] is also a significant problem in some structures because of forces involved in drying the structures after release. This has led to special release procedures.

Both hybrid and monolithic mixtures of transducers and readout circuitry are now being used, with a trend toward monolithic implementations as processes become better understood. Certainly for high-volume applications, the monolithic approach is attractive since added process development costs can be recovered, final cost is somewhat lower, and reliability may be improved in the absence of internal wire bonds. Even here, however, it seems likely that the integration levels on transducer chips will remain modest, with more complex digital signal processing and/or microprocessing done as a separate in-module IC. This reflects the current approach in

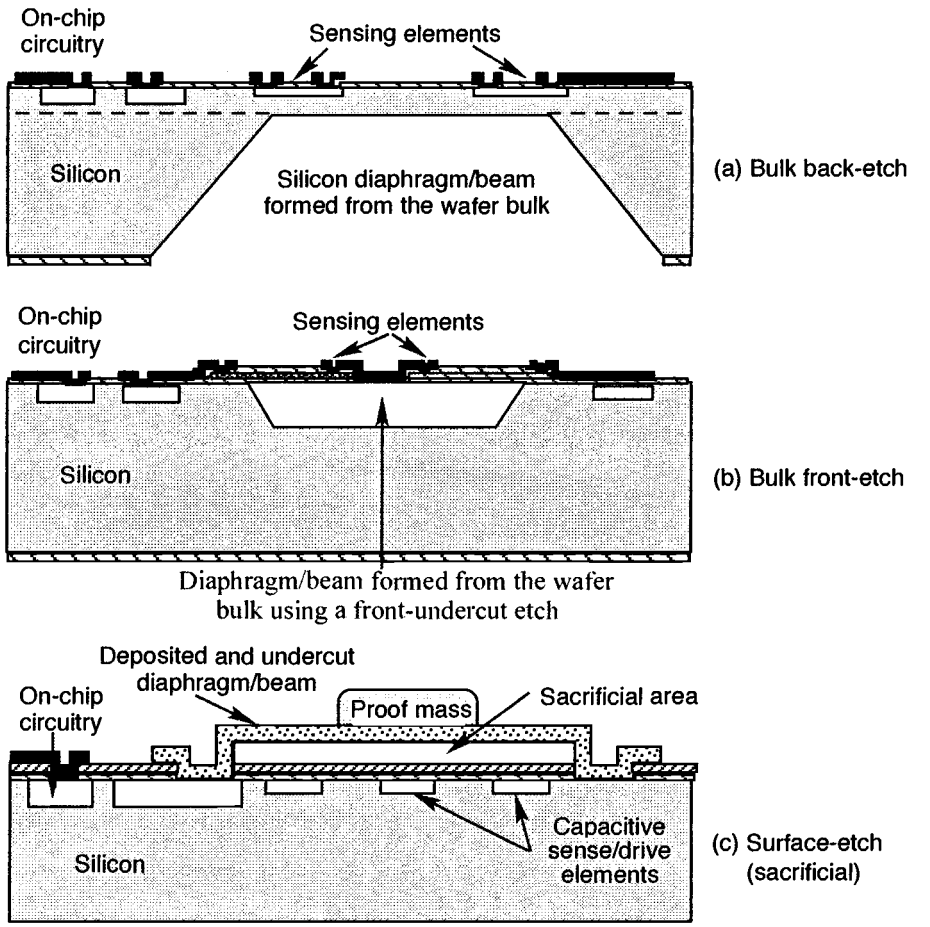

Fig. 10.7. Comparison of bulk, front-undercut, and surface micromachined-device structures.[4]

the μCluster. Bulk micromachining typically requires the formation of etch-stops prior to the circuit fabrication sequence, whereas surface micromachining requires the addition of the microstructures after the normal circuit flow. In either case, well-designed circuitry can go a long way toward making a marginal transducer look good. Surface-micromachined structures based on lateral capacitance, for example, may have full-scale capacitance ranges of no more than 100fF, making it a real challenge to achieve a broad analog output range. Bulk microstructures can do significantly better but are somewhat more difficult to merge on-chip with circuitry.

10.6.3.3 Representative Devices

A wide variety of sensors and actuators are in development, and during the next 5 years many of these are expected to move to commercial production. Indeed, the worldwide annual market for such devices is expected to increase several fold during the coming decade, reaching into the tens of billions of dollars. The present μCluster contains sensors for pressure, temperature, humidity, and acceleration (both threshold [impact] and continuous [tracking]), with additional sensors for acoustic and chemical analysis in development. In this section, we will look at the barometric pressure sensor as an example of a device currently in the μCluster and will then mention briefly an IR (thermal) sensor and a gas detector as other examples of emerging devices.

10.6.3.3.1 High-Resolution Barometric Pressure Sensor

Micromachined, silicon pressure sensors employing dielectric or silicon diaphragms can be grouped according to their transduction mechanism as piezoresistive or capacitive and according to their readout structures as static, resonant, or tunneling devices. In spite of impressive recent progress in sensitivity and accuracy, emerging applications in environmental monitoring offer substantial challenges in that they demand both high accuracy and a wide operating pressure range in order to precisely resolve the local pressure differences needed for global weather forecasting. With a desired resolution of about 25 mtorr (equivalent to about one foot of altitude shift at sea level) over a dynamic pressure range from 500 torr to 800 torr, this amounts to resolving nearly 1 part in 10^5 over a temperature range from perhaps –25°C to +60°C. In this section, we illustrate an approach to meeting these needs.

Figure 10.8 shows the structure of the barometric pressure sensor.[57] This device is composed of four capacitive pressure-sensing elements, each formed with a bossed diaphragm and a readout electrode on an opposing glass substrate. The diaphragms and bosses are both circular to avoid high stress concentrations. Since the bosses are much thicker (12 μm) than the diaphragms (2 μm), most bending and stretching when exposed to differential pressure occurs in the thin diaphragm. The bosses act as parallel plates with respect to electrodes on the glass substrate. These electrodes serve as reference plates, and the diaphragms suspended over them act as movable plates, forming pressure-variable capacitors. Since this sensor is intended for use in the μCluster, it is important that the device be physically small and dissipate very little power.

The device is vacuum sealed, so barometric pressure deflects the diaphragm downward toward the reference electrode on the glass. The capacitance is inversely proportional to the gap distance between the boss and the reference electrode so that the capacitance and pressure sensitivity increase rapidly as the plates approach each other. However, the operating range of the device becomes very limited since the plates soon touch as the pressure increases. A series of diaphragms having slightly different diameters will deflect different amounts due to barometric pressure, however, and will hence cover different portions of the overall measurement range. As the plates touch, ending one measurement segment, the glass provides a built-in strain relief for that device, and the next smaller diaphragm will move down into the working gap range, continuing the measurement into the next higher subrange in pressure. Figure 10.9 summarizes this device operation. The 9.5-μm zero-pressure gap is reduced to a working distance of 0.4–0.7 μm over the pressure range of interest.

Atmospheric pressure is first measured using a pressure sensing element (S1) that is designed to cover a broad operating range (500–1000 torr ± 1 torr). Depending on this reading, one of the

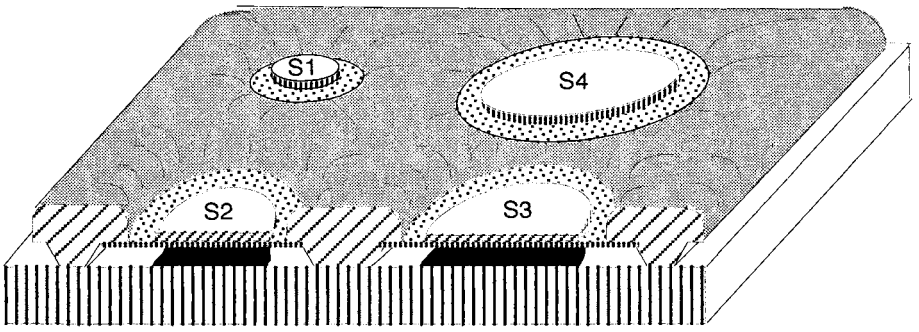

Fig. 10.8. The overall structure of the multi-element barometric pressure sensor.[4]

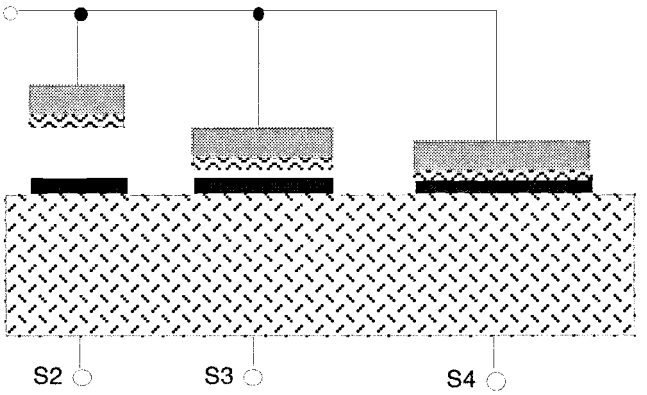

Fig. 10.9. Sensor operation. The multiple sensing elements of a device under a typical working condition are shown. The center device would be used for measurements here.[57]

other sensing elements is then selected to provide a higher sensitivity look at that particular subrange (e.g., 600–650, 650–700, or 700–760torr). The other pressure sensing elements will either have a larger gap separation or will be touching and hence strain relieved, as shown in Fig. 10.9. The capacitance of the selected element is read out using a switched-capacitor integrator[58] (Fig. 10.10) whose output is digitally compensated for temperature and nonlinearity effects. The switched-capacitor interface circuit is integrated in a 3-μm CMOS process on a 2.2 × 2.2-mm chip that also provides command decoding, control, temperature sensing, and interfacing through a sensor bus to the embedded microcontroller.[59] The pressure sensors are self-testing, using the applied electrostatic voltage derived by lengthening the readout pulse width.[58]

The pressure sensor is fabricated using a five-mask, silicon-bulk-micromachined, dissolved-wafer process[60] with a die size of 5 × 6 mm. The silicon processing starts with a p-type (100) oriented silicon wafer of normal thickness (550 μm). A KOH etch is first performed to define a recess that will later provide the capacitor gap, connecting channels among the different elements and the tunnels for the output leads. The KOH etch time and temperature determine the depth of

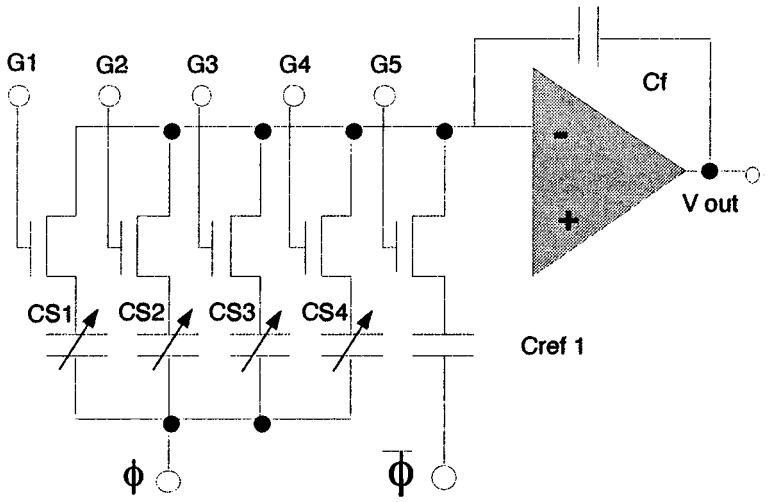

Fig. 10.10. The switched-capacitor integrator used for measuring the transducer output capacitance as a function of applied pressure.

the recess (nominally 9.5 μm). Note that this depth is not particularly critical, since by adding segments on either end of the measurement range, gap variations from device to device can be accommodated. Photolithography is next used to define the supporting rim and the center bosses, which are diffused to an etch-stop depth of 12 μm. The thin (2-μm) portion of the diaphragm is then formed using a shallow boron diffusion. A layer of LPCVD SiO_2 is then deposited and patterned on the diaphragm to prevent electrical shorts when the capacitor plates touch as well as to compensate the diaphragm internal stress associated with the boron diffusion. The glass processing consists of metallization to form the reference electrodes and the drilling of an optional hole in the glass substrate for use in vacuum sealing. Once the silicon and glass processing are completed, the silicon and glass wafers are electrostatically bonded together. The silicon wafer is then etched away in EDP, leaving only the heavily boron-doped areas on the glass. While a batch vacuum-sealing process involving deposited materials at wafer level has recently been developed,[60] the present devices used in the μCluster were sealed by first sealing the lateral lead tunnels and then placing the devices in a vacuum chamber subsequently evacuated to a pressure of less than 1 torr. A pass-through arm was then used to apply a vacuum sealant to the vent hole in the substrate. The sealant was then cured in vacuum.

Figure 10.11 shows the measured (uncompensated) pressure response for the "global"-sensing diaphragm, which spans the measurement range from 500–800 torr. It has a nearly linear, capacitance-pressure output characteristic with a pressure sensitivity of about 2 fF/torr (420 ppm/torr). Figure 10.12 shows measured responses from three of the other device elements. The sensing element having the largest diaphragm size gives output readings over a pressure range of 600–650 torr. The sensing element with the next smaller diaphragm size provides output in a pressure range of 650–700 torr, and the smallest diaphragm responds from 700–750 torr. Pressure sensitivities for these "segment" diaphragms are about 25 fF/torr, corresponding to about 4200 ppm/torr or equivalent to a resolution of about 1-ft altitude near sea level.

The barometric pressure sensor illustrates the utility of an embedded microprocessor along with software control, forming an integrated microsystem. The approximate pressure can be read

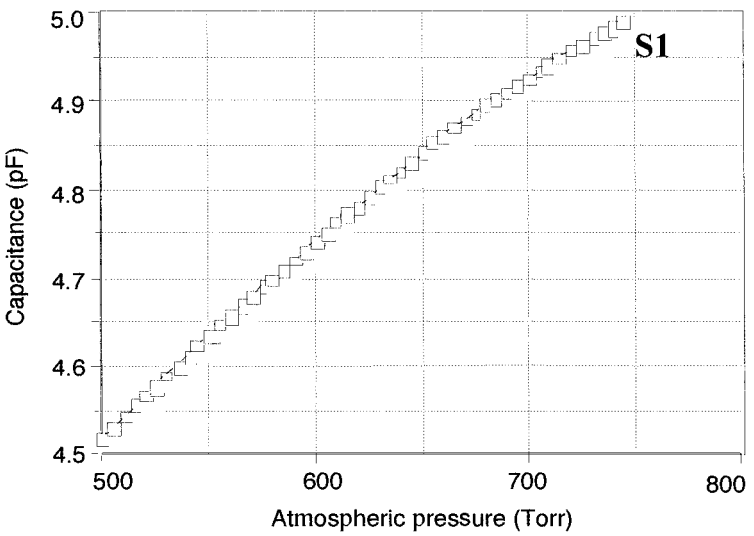

Fig. 10.11. Response of the global transducer spanning the overall barometric pressure range of the device. The pressure sensitivity is about 2 fF/torr

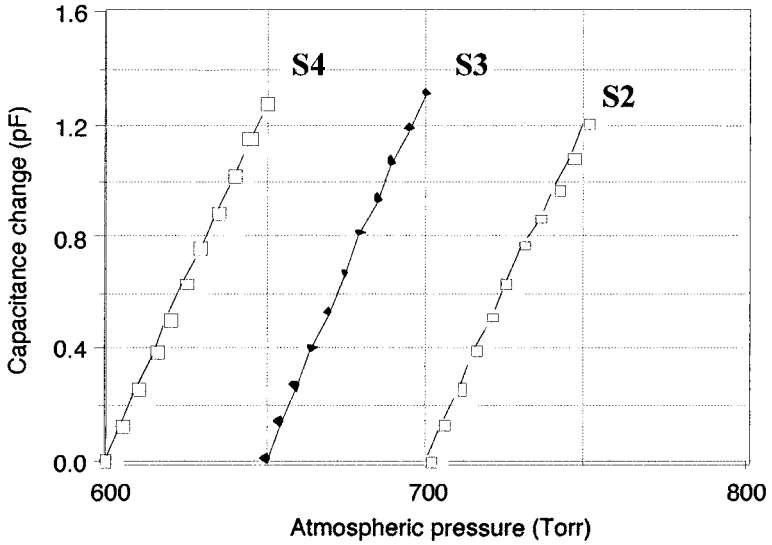

Fig. 10.12. Measured responses from the higher-resolution (segment) sensing elements. The pressure sensitivities are about 25 fF/torr.

using a global sensor, and a more exact reading can be obtained using the appropriate segment device. Digital compensation of the measured output allows an order-of-magnitude more resolution and accuracy than would laser trimming, and self-testing is possible to a considerable degree. Similar strategies can be employed for a broad range of other devices in such systems, including the following examples.

- Broad-range temperature sensor arrays
- Programmable frequency-range vibration accelerometers
- Broad-spectrum acoustic sensors
- Cross-correlated chemical identification devices and biological agent detectors

10.6.3.3.2 Micromachined Infrared Sensors

Throughout the 1970s and most of the 1980s, most work on IR imaging devices was done using compound semiconductors or silicon Schottky diode arrays operated at liquid nitrogen temperatures. While adequate for some applications, the cooling requirement made such devices inappropriate for most commercial applications. By the mid-1980s, however, silicon micromachined imagers capable of operating at ambient temperature had been demonstrated for process control applications,[43] and by the early 1990s higher-density imagers were emerging targeted at night-vision applications.[44] Figure 10.13 shows the cross section of one of the early imagers. This device uses a dielectric window for thermal isolation between an array of series-connected hot junctions and an array of cold junctions located on the chip rim. When incident radiation falls on the array, the hot junctions are warmed and the thermopile converts the temperature rise into an electrical output. Such devices allow a remote temperature resolution of better than 1°C with a thermal time constant of a few milliseconds and typical responsivities of 50–100 V/W using windows measuring 400 μm on a side. Such pixel sizes are adequate for process control, but do not permit the numbers of windows required for night-vision applications. More recently, surface micromachining has been used to realize much denser arrays having pixel sizes of 50 μm on a side with responsivities as high as 70,000 V/W and a typical noise-equivalent temperature

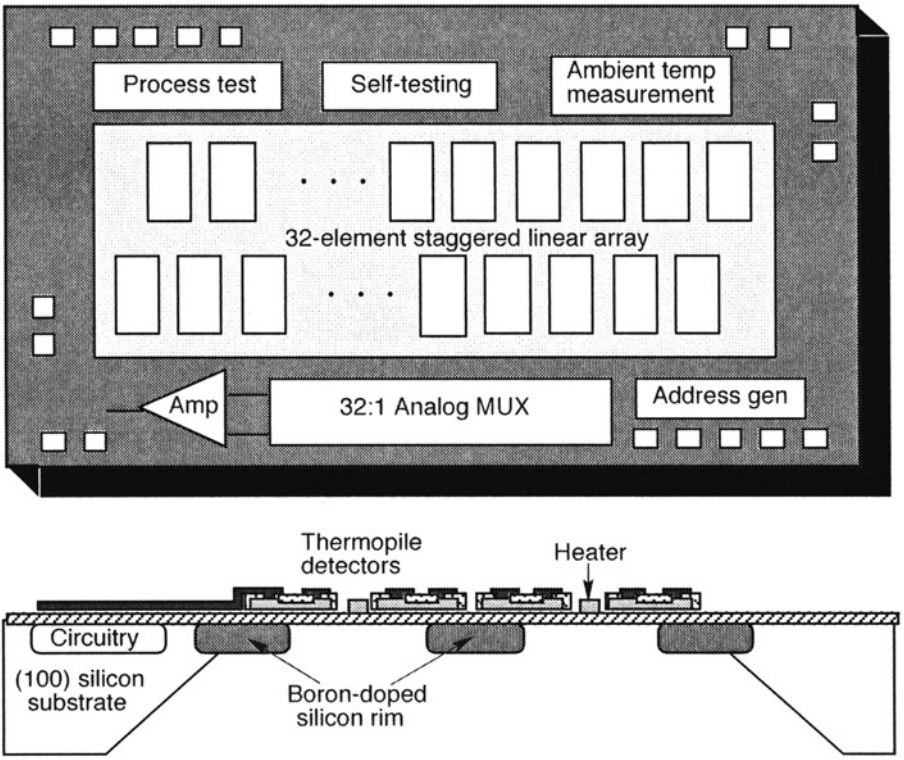

Fig. 10.13. Top view and cross-section of a micromachined thermal line imager. Thermocouples are supported on dielectric windows where the hot junctions are heated by incident radiation, converting input power into an electrical output.[61]

difference (NETD) of about 0.05°C.[43] Imagers composed of 80,000 pixels have shown excellent night-vision capabilities while operating at ambient temperature. Finally, active-pixel micromachined arrays using heated arrays with local feedback within the pixels have reported responsivities of more than 10^6 V/W.[62] Such arrays should find important applications in both ground- and space-based applications.

10.6.3.3.3 Micromachined Gas Sensors

One of the more promising approaches to chemical (gas) sensors is based on the structure shown in Fig. 10.14.[63] A dielectric window is again used, this time with a bulk micromachined silicon heater under it. On the top side of the structure is a thin deposited film (e.g., 35 Å-Pt on 50 Å-TiO_x) along with four electrodes to allow accurate measurement of its resistance. With an appropriately prepared film, gases such as oxygen and hydrogen can be detected with ppm accuracy. By accurately controlling the film temperature and ramping it over a predetermined range, temperature-programmed desorption (TPD) can be used as an aid in determining the gas or gases present. Microcalorimetry effects can also be employed for gas analysis in such structures. While selectivity remains a problem in these devices, a common approach is to use an array of dielectric window detectors with each one coated with a different conducting film so that the array produces a unique signature for a given gaseous mixture. Embedded microprocessors and/or neural networks can then in principle be used to deconvolve the signature to specify a unique gas

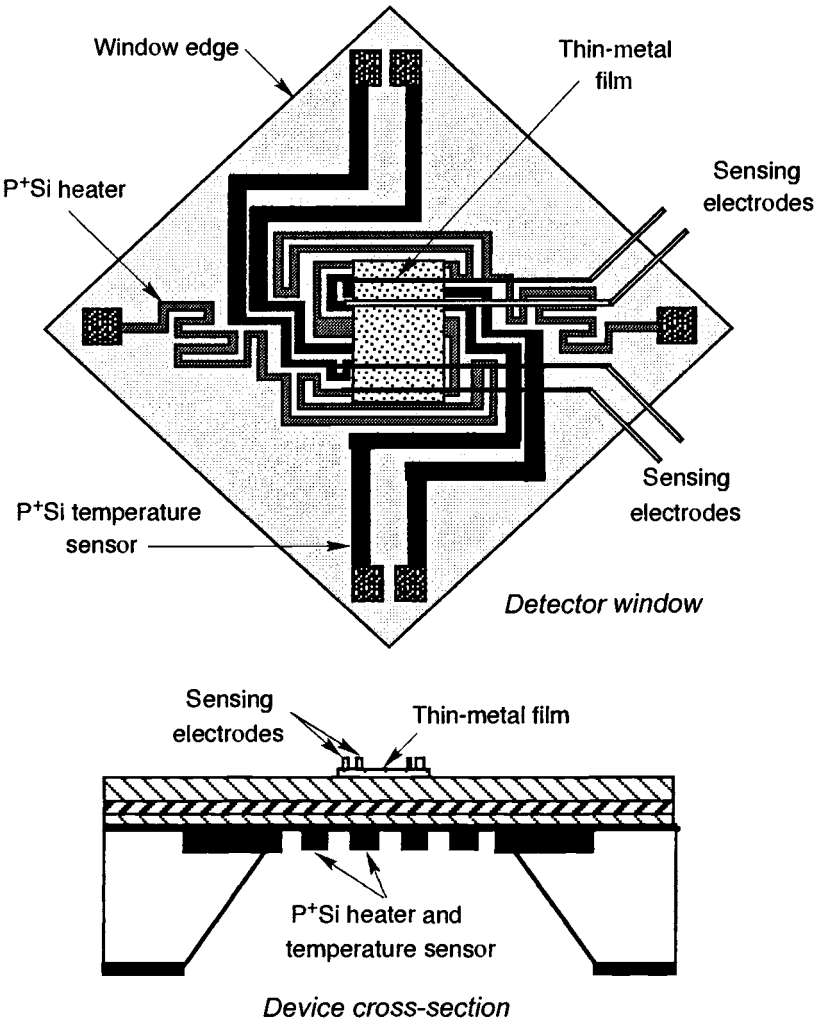

Fig. 10.14. Top view and cross-section of a micromachined gas detector. The device employs a heater suspended under a dielectric window. A thin film on top of the window changes its conductivity in response to gas adsorption from the surrounding environment.[63]

composition. Thus, such arrays are promising candidates for use in microsystems. Power must be conserved as much as possible in battery-powered applications by pulse-heating the windows, which have typical thermal efficiencies of 6°C /mW in air. It is significant that detector films can be deposited using chemical vapor deposition (CVD) by placing completed arrays in an appropriate gas stream and selectively heating the desired window to catalyze film growth.[64] The electrodes, which are already in place, can be used to terminate growth at the appropriate film resistance. This technique allows an array to be effectively programmed for a given application.

A still more versatile approach to analyzing gaseous mixtures can be based on gas chromatography. A number of research efforts focus on miniaturizing such devices using micromachining. As shown in Fig. 10.15, a series of microvalves forms a gas-sampling system that allows a sample of unknown gas to be injected into a carrier gas stream. As this sample passes through the column,

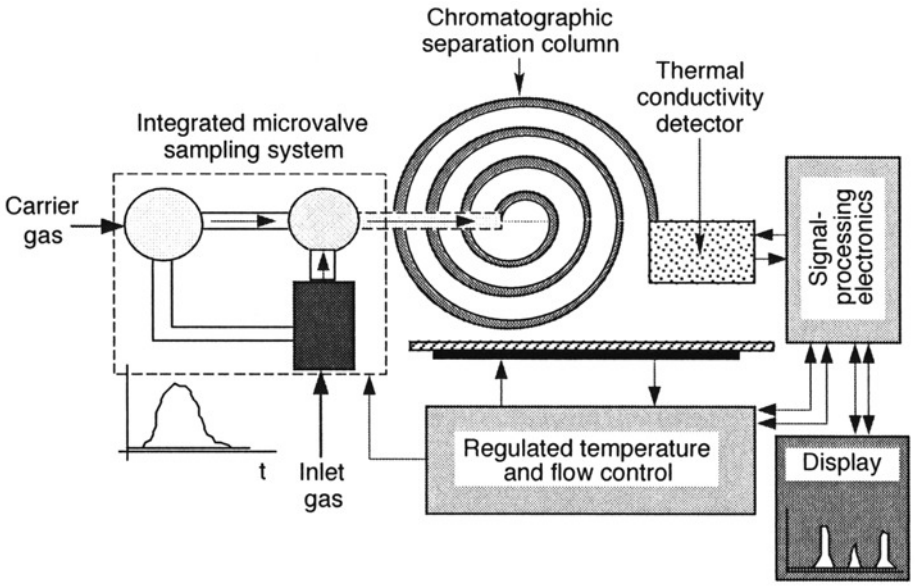

Fig. 10.15. Block diagram of an integrated gas chromatograph. A sample of unknown gas is injected into a carrier and passed through a long capillary tube, where the different molecular species are separated in time. Emerging gases are detected using a thermal conductivity detector and identified as to type by their characteristic delays. The amount of gas present can be determined from the integral of the detector response.[65]

different molecules spend different amounts of time stuck to the walls of the column, so that at the far end of the tube they emerge separated in time. They can then be detected using thermal conductivity sensors or by other means. While the first silicon gas chromatograph was reported almost 20 years ago,[66] microvalve technology at that time did not allow the realization of a fully integrated microsystem. Over the next few years, such microinstruments should emerge, and if incorporated within a microsystem unit such as the μCluster, should find wide application in military and civilian applications.

10.6.4 Other Components and Features of the μCluster

10.6.4.1 Sensor Bus

An important aspect of the μCluster's generic architecture is the standard sensor bus, which establishes a fixed mechanism by which the controller can communicate with the sensor network within the microsystem. Although a variety of network standards is available for use as the sensor bus, the one chosen for the μCluster is based on the Michigan Serial Standard[67] and was selected because it provides the necessary features while minimizing the number of signals and complexity of the bus. This, in turn, minimizes both the electronics required for interfacing to the bus as well as the trace count to reduce package size. Because it plays a significant role in the microsystem and affects many aspects of system operation, the sensor bus is discussed in detail in this section.

As shown in Fig. 10.16, the μCluster's sensor bus consists of three power lines, four signals for bidirectional serial communication, a shared data line for sensor output, and a data valid/interrupt signal. The three power lines are the ground reference (GND), the main system power (VDD), and a switched 5-V reference supply (VREF). VDD is defined as 6 V to be compatible with common battery voltages. This supply is on constantly while the μCluster is active. VREF,

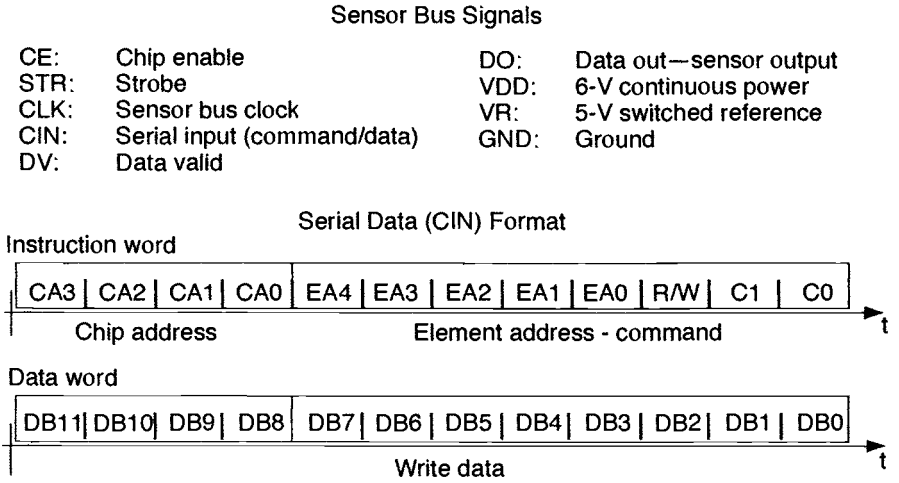

Fig. 10.16. The μCluster sensor bus provides a standard for communication between the controller and the front-end sensor network. Shown are the signal lines that make up the sensor bus as well as the format for the serial data used to issue instructions to sensors on the μCluster.

on the other hand, is switched on and off as part of a power-management scheme discussed in Subsec. 6.4.4.4. VREF is part of the sensor bus so that electronics on the sensor front end can be turned off when not in use. VREF is a 5-V reference that will remain constant even as the battery voltage, VDD, decreases over time. A constant reference voltage is necessary for the analog readout circuitry on the sensor front end. The sensor data output signal (DO) is shared by all sensor modules in the microsystem and multiplexed by the modules themselves. That is, each sensor module will have its output disabled from the DO line unless commanded by the controller to put data on the line. Data on the DO line can be in the form of an analog voltage, a serial bit stream, or frequency-encoded data (provided the controller can handle each of these formats). The data-valid (DV) signal is used to let the controller know when valid data is available on the DO line. DV also doubles as an interrupt that can be used to request communication with the controller as part of, for example, an event-triggered response. Use of the DV interrupt provides the μCluster with the capability of on-demand sensor readings rather than being limited to simple preset sensor scans.

The four serial communication signals on the sensor bus are a chip-enable signal (CE), a data strobe (STR), a serial data line (CIN), and a clock (CLK) signal. A timing diagram for these serial communication lines is shown in Fig. 10.17. Because of the nature of the sensor bus, communication can only take place with one front-end sensor module at a time. When active (high), the CE signal indicates that the sensor bus is in use by a specific sensor module so that no other module can interrupt the system until this line goes inactive (low). The STR signal defines a window around the commands being sent from the controller to a specific sensing node so that bus interface hardware will know when a message begins and ends. Used in combination, the CE and STR signals tell the sensor modules when they should be reading or ignoring incoming data. Command and data bits sent from the controller to the sensor modules are placed on the CIN line, and the bits are synchronized to the CLK signal so that they can be easily read by bus interface hardware. The data format for information on the CIN line is shown in Fig. 10.16.

At the beginning of a communication from the controller, the CE bit goes high, and a 4-bit chip address is put out on the serial data line, CIN. Each sensor module has a predefined chip address

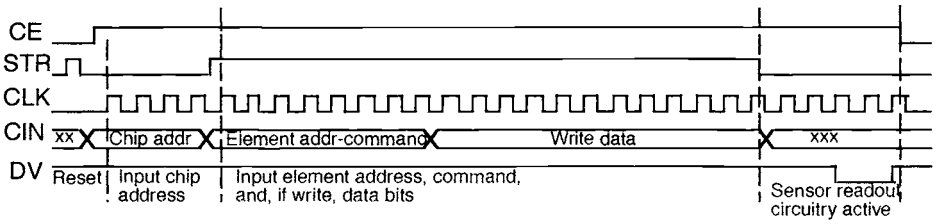

Fig. 10.17. Timing diagram of the serial communication signals on the sensor bus.

and will only listen to a message if it begins with a matching chip address. At the end of the chip address, the STR line goes high to mark the beginning of a sensor-specific message. This message begins with a 3-bit command code followed by a 5-bit element address. The 5-bit element address can be used to access up to 32 readable elements (e.g., sensors) and 32 writable elements (e.g., actuators, digital registers) per sensor module. This format allows multiple sensors to share the same bus interface hardware, or allows each element in a multielement sensor array to be accessed individually. If the command is a write instruction, data bits follow the element address to be stored or used directly by the sensor interface circuit. At the end of this message the STR signal will go low. If the command is a read instruction, the sensor readout circuitry must convert the sensor data into one of the possible output formats. During this time, the CLK line is available to the readout circuitry and can be programmed to any frequency and duration (limited only by the controller generating the clock signal) as required by the specific readout circuitry. Once the readout is complete, the bus interface hardware places the data on the DO line and indicates that valid data is available by pulling down the active low DV line. Once the data has been read by the controller, the CE line goes inactive to reset the bus interface hardware and disable the output on the DO line. At this time the controller can either monitor the DV line for an interrupt or initiate another communication to a sensor module.

The sensor bus described is a generic form. For use on the μCluster, a more specific implementation was developed, for which appropriate command codes and element address bits were defined and a corresponding bus interface circuit was designed. The bus interface circuitry was implemented as part of the Capacitive Sensor Interface Chip (CSIC) that includes additional circuitry for the readout of capacitive sensors and an on-board temperature sensor.[59] A block diagram of the CSIC is shown in Fig. 10.18. For application with the μCluster and the CSIC, the 3-bit command code is used to define one of five command options implemented by the CSIC. Of these commands, one is a read instruction and the other four are write instructions that access different data registers, including a 4-bit Chip Command Register (CCR). The CCR is a 4-bit, on-chip control register that can be accessed without writing to a specific element address. This reduces hardware overhead and simplifies setting the four primary control bits used by the sensor readout circuitry. The sensor readout circuitry on the CSIC is a three-stage switched-capacitor circuit[68] that can convert capacitive sensor data into an analog voltage read by the microsystem controller. This circuit uses the five-bit element address to determine which of six possible sensor inputs will be read and which of four possible reference capacitors will be used during the data conversion. The on-chip reference capacitors provide programmable offset control and allow the CSIC to be used with sensors that have nominal capacitance in the range of 1 pF to 12 pF. The multiplexed sensor inputs allow one CSIC to be used with up to six sensing elements. The CSIC also has programmable gain settings that use the bits of the CCR to control the gain of the sensor readout circuit. The programmable gain allows the CSIC to accommodate sensors with a wide range of sensitivities. The final block of the CSIC is a simple temperature sensor formed by a ring

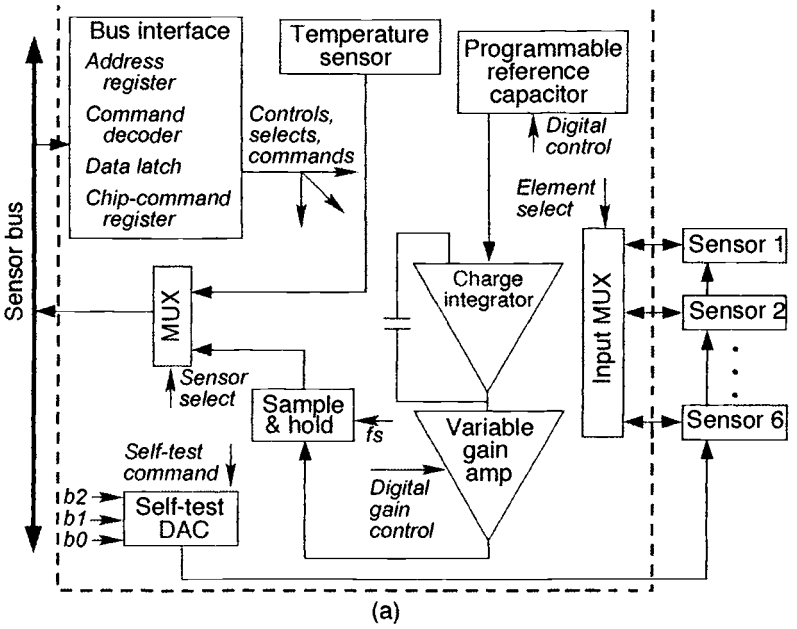

(a)

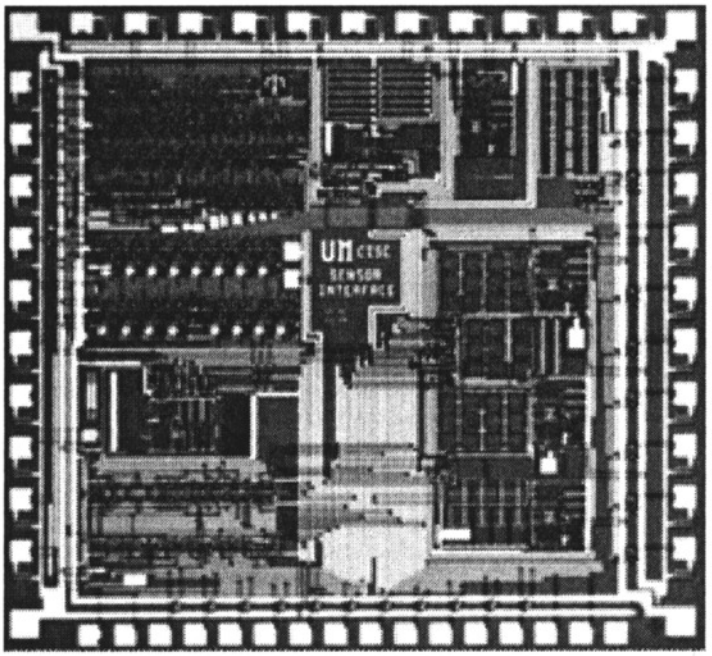

(b)

Fig. 10.18. (a) Block diagram of the Capacitive Sensor Interface Chip (CSIC). CSIC includes circuitry that will interface to the sensor bus, readout multiple capacitive sensors, and measure the temperature of the chip and its surroundings. (b) Photograph of a fabricated CSIC die, which has been laid out approximately as shown in the diagram.

oscillator with an output frequency that varies with temperature. The temperature sensor on the interface chip provides an accurate measurement of the temperature in close physical proximity to other sensors on the μCluster. This makes the temperature sensor very useful for digital compensation of temperature sensitivities in other sensors as discussed in Subsec. 10.7.4.

10.6.4.2 Microcontroller

As discussed earlier, a large variety of commercially available controllers may be used in microsystem applications. For use with the μCluster, the Motorola 68HC711E9 Microcontroller Unit (MCU) was chosen as the best of the available alternatives because it offers the following features on a single 8 × 10-mm die:

- An 8-bit microprocessor
- An 8-bit analog-to-digital converter
- Timing hardware
- A synchronous serial peripheral interface (SPI)
- An asynchronous serial communications interface (SCI)
- Built-in memory: 512 bytes RAM, 512 bytes EEPROM, and 12 kbytes EPROM
- Low-power mode

Each of these features is necessary in order to be compatible with the goals and requirements of the μCluster:

- The microprocessor is needed to execute control software that can be stored in the on-chip memory.
- The A/D and timing hardware are necessary to read out sensor data in the analog and frequency-encoded formats provided in the sensor bus definition.
- The SPI allows for high-speed serial data transfer across the sensor bus with minimal software overhead.
- The SCI is a universal asynchronous receiver transmitter (UART) type interface that provides a well-known standard for communication between the microsystem and external host system.
- In addition to storing control software, the on-chip memory includes EEPROM, which is very useful for storing sensor-specific data within each microsystem
- The low-power mode available on the 68HC11 MCU is vital in minimizing the power consumption of the μCluster.
- The 68HC11 is available in die form necessary for the multichip module packaging used for the μCluster.

Many other available controllers offer some, but not all, of these required features. However, as the popularity of microsystems grows in the coming years, manufacturers are sure to answer the demand with other controllers that offer these features and more. There already is evidence that new controllers are being specifically designed for sensing systems. The limiting aspects of the 68HC11 are its 8-bit architecture, relatively slow speed (a maximum bus speed of 2 MHz), and the 8-bit A/D. There is a need for a wider processor word (e.g., 16 bits) and higher A/D accuracy (≥12 bits), but these advances need to be achieved while reducing the overall power dissipation. This performance may be possible if the generality of the processor is reduced to eliminate unneeded functions, emphasizing the sensing/control functions discussed here.

10.6.4.3 External Communication

Although a primary goal of the μCluster is to utilize wireless communication so that the host system can receive data from a remote site, it is also important to have a hardwired interface to the external world. The hardwired interface is useful for developmental purposes since it allows the

user to program the controller and examine and debug system operations easily. It is also useful in many applications where a hardwired link is preferred because it eliminates the need for a matching receiver to the wireless transmitter. In the design of the μCluster, it was only necessary to provide wireless data output, so all inputs utilize a hardwired interface. Since both a wireless and hardwired link will normally exist, the two links should be as similar as possible. Using a well-known standard for external communication will minimize the interface hardware necessary between the μCluster and the host system.

Given these guidelines and the fact that the MCU chosen for the μCluster has a built-in RS-232-compatible UART type interface, the asynchronous serial RS-232 format was chosen for external I/O. For direct connection to the serial port of a common PC, only a widely available level-shifter buffer is needed to convert the 6-V signals of the μCluster to the 12-V levels of the PC. This standard was chosen more for its simplicity than its functionality. Indeed, there are many other network standards available that may be more appropriate for a given macrosystem. Note that the RS-232 does not limit the μCluster to a macrosystem based on this network scheme; an external network conversion interface could be used to convert the RS-232 format to an alternate network protocol without affecting the inner workings of the μCluster.

For the wireless transmitter, the HX1005 by RFM, Inc., was selected. This component has typically been used for keyless entry systems in automotive applications. The advantages of this component were its small size and low-power consumption, which were found to be more compatible with the demanding goals of the μCluster than other commercial components. The HX1005 is an RF transmitter with a carrier frequency of 315 MHz and is compatible with the UART communication interface chosen for data output from the μCluster. By using amplitude-shift-keyed modulation, the same data sent to the UART could be directed to the transmitter for wireless data output. Data at the receiver end can be easily converted to an RS-232 format. This makes the method of data transfer, whether hardwired or wireless, transparent to the host system. The range of transmission from the μCluster using the HX1005 is largely dependent on the receiver and the type of antenna used. A range of more that 100 ft has been observed using a low-power receiver that runs off of four AA batteries. Greater range can be obtained at the cost of increased power, both on the μCluster and at the receiver.

10.6.4.4 Power Management

A primary goal of the μCluster was to provide all desired sensing functions while minimizing power consumption. Options for managing the power consumption can be reduced to two approaches: minimizing the power consumption of each component in the microsystem and keeping all unnecessary components turned off until needed. The first of these is relatively simple from a system point of view: choose components for each functional block that have the lowest possible power consumption. Of course, this may mean facing difficult trade-offs in performance that have to be analyzed thoroughly. Most of the difficult issues in this area are faced in the design of the individual components and, as such, are beyond the scope of this chapter. It is worth noting, however, that capacitive sensors provide a tremendous advantage over piezoresistive devices since the only power they consume is that of the readout circuitry, which can be minimized by careful design. For this reason, the pressure, humidity, and acceleration sensors used on the μCluster are all capacitive.

In the second approach—keeping all unnecessary components turned off until needed—power management becomes more of a system issue. Power management is addressed in the sensor bus, which includes a voltage reference that can be switched off when the sensor front end is not being used. If there are sensors or subsets of sensor nodes that need constant power, there is also a

supply voltage on the sensor bus that is always on. The μCluster has an advantage here over some other sensing systems in that most of the parameters being measured have very low bandwidth and as such do not need to be monitored often. Measuring barometric pressure, relative humidity, or temperature can be done, for instance, once a second without significant loss of relevant data. However, in the case of acceleration, which can generate signals with significantly broader bandwidth, an alternate approach is necessary. Again the sensor bus provides for this by allowing for event-triggered interrupts between normal sensor scans. Using this feature, a threshold accelerometer, which sets a mechanical switch when an acceleration beyond a certain threshold is experienced, can be used to interrupt the controller and request an immediate reading of a more accurate on-board continuous accelerometer.[69] Thus, only a low-power digital circuit that monitors the threshold device and generates the interrupt needs to be on continuously. A similar approach can be used by many other sensors that might normally be too power hungry for such low-power systems as the μCluster.

In addition to switching off the sensor front end between sensor scans, it is also necessary to minimize the power consumption of the MCU, which in the case of the μCluster is, by far, the largest power consumer in the system. Since the sensing activities of the μCluster are of very low frequency, there is a large block of time between sensor scans when it is not necessary to have the MCU running. As long as some circuitry monitors the sensor-bus interrupt signal, the MCU can be shut down just as the sensor front end is. To accomplish this, the built-in MCU low-power mode is utilized. In this mode, the clocks on the MCU are shut off, all outputs are latched to their current values, and data in RAM is maintained, while the power levels are reduced by three orders of magnitude. A similar mode is available on many controllers. The disadvantages of this mode are that the MCU is nonfunctional, and it must be restarted by an external signal. It is therefore necessary to include some control circuitry external to the MCU that will monitor microsystem activities while the MCU is in low-power mode and will wake the MCU after the appropriate delay.

A power management chip (PMC) was developed for use in the μCluster to accomplish this task. The PMC has on-chip clocking circuitry that is activated by the MCU before it enters its low-power mode. The MCU sends a code to the PMC that defines the desired delay, which can be one of eight discrete values between 15 s and 5 min. After this, the MCU goes to sleep and the PMC is in control until the delay time is over. During this delay it is necessary for the PMC to monitor the sensor bus in case an event-triggered interrupt is generated. When either an interrupt is received or the delay time expires, the PMC wakes the MCU, which takes back control of system operations.

A block diagram of the PMC is shown in Fig. 10.19. As shown in this illustration, the PMC also contains switching circuitry that controls the delivery of power to other areas of the system. These switches are set by inputs from the MCU, and they control whether the transmitter gets power and whether the 5-V reference of the sensor bus is on or off. The 5-V reference is implemented with an Analog Devices REF-195. This component is compatible with the goals of the μCluster and is available in die form. The PMC is, in a sense, an extension of the MCU, under its direct control, and used to control and minimize the power consumption of the μCluster.

10.6.5 Summary of Microinstrumentation Cluster Design

Having defined a generic microsystem architecture and discussed many aspects of the components to be used in one specific realization (the μCluster), we will review some of the trade-offs encountered and the decisions affected by some choices. Designing the μCluster began with determining a generic microsystem architecture and defining a standard sensor bus. Both aspects

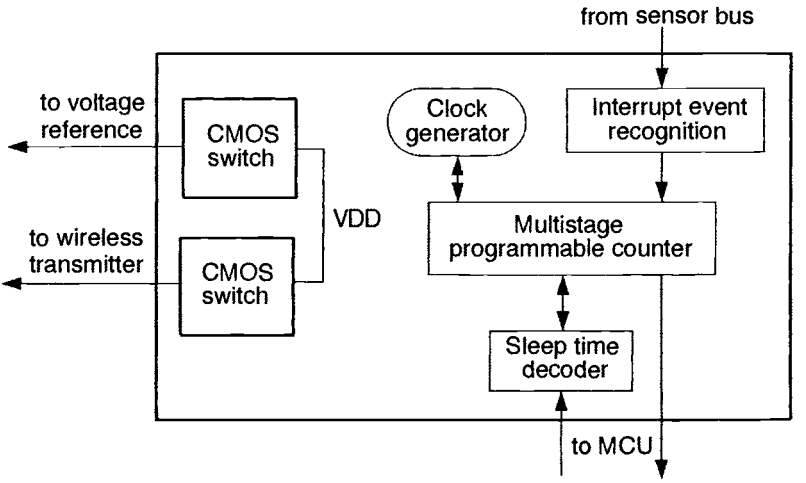

Fig. 10.19. Block diagram of the power-management chip used to control power flow across the μCluster and monitor system activities while the MCU is in low-power mode.

placed specific requirements on the microsystem controller, which is important to select early in the design because many other design choices relate to this component.

The controller had to communicate across the defined sensor bus for intramodule operations and across an external network bus for interaction with a host system; it had to read analog, digital, and frequency-encoded data from the sensor front end; and it required a nonvolatile memory device in which to store control software and sensor variables. Although these functions could be obtained by separate electronic components, it is much better if they are built into a single controller, especially when size is an issue. Once a controller that met these requirements was selected, the sensor interface circuitry could be designed.

The sensor readout circuitry on the interface chip was designed to meet the requirements of several MEMS transducers already under development for measuring the targeted environmental parameters. After designing the sensor-interface circuitry, the transducers could be modified, if necessary, to meet the interface circuit requirements. For example, the nominal capacitance of the transducer had to fall into the range supported by the sensor readout circuitry on the interface chip.

Meanwhile, as iterations between interface circuitry and transducers were being made, other system-level issues such as power management and external I/O could be addressed. Determining the appropriate power-management schemes revealed that hardware in addition to the controller would be necessary. The power-management chip was then designed, and a commercial 5-V reference selected. These two components contain the necessary control circuitry outside of the controller itself.

At the same time that the power-management chip, the sensor interface chip, and the transducers were being designed and fabricated, the wireless link was investigated. After an initial attempt to design a custom transmitter failed to meet the size and power budget of the μCluster, a commercially available alternative was sought. The transmitter had to be compatible with both the power levels available on the μCluster and the inputs possible from the chosen controller. With the identification of an appropriate component, the design phase was complete. Making a complete system out of the various components is the subject of the next section.

10.7 Fabrication and Testing of the μCluster

10.7.1 Fabrication

Fabrication of a complete microsystem such as the μCluster involves many different efforts. Organizing these efforts so that work can be performed in parallel provides greater efficiency. While some of the specific tasks may vary with the project, the plan for fabrication of the μCluster provides a good example of how to structure the necessary efforts. Figure 10.20 shows a time-based production map of the activities in constructing the prototype microsystem. The activities are divided into three primary functional efforts dealing with the sensor front end (transducers and interface electronics), the system hardware (MCU, I/O, etc.), and software. They cover the project from basic transducer and electronics design to overall system operation, packaging, and testing. Because different people were responsible for different aspects of the project, the map is useful in illustrating the interrelation of activities and the order in which tasks must be completed.

At the beginning of the map in Fig. 10.20 are activities such as design, fabrication, and selection of the components that form the μCluster. Selection of the MCU directly relates to many of the other tasks, including, in this case, the design of floating-point math software routines to provide more accurate calculations than normally allowed by an 8-bit microprocessor. Near the middle of the map, all the components are available, including a set of "known good die" for the custom devices used. The later part of the map shows the final development of a prototype unit with packaging and testing. After the prototype is checked, and assuming that no redesign is

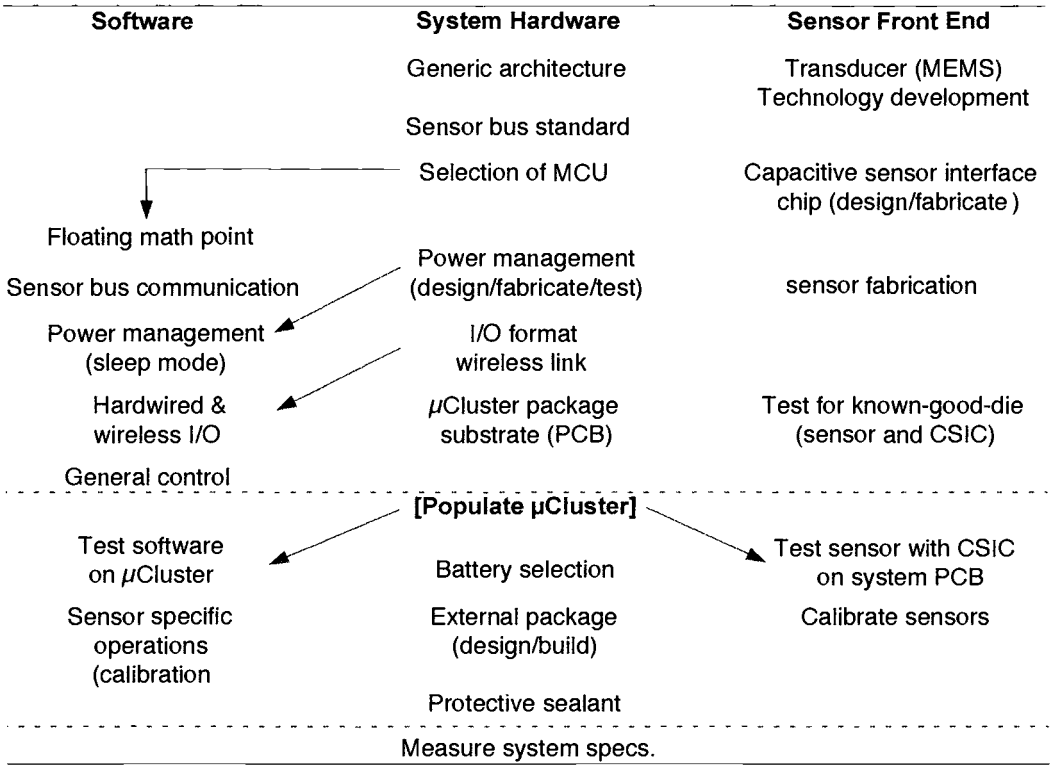

Fig. 10.20. Map of tasks to be performed during the fabrication of the μCluster. The tasks are mapped from top to bottom in the order they must be completed. The interrelation of parallel activities are indicated by arrows connecting the tasks.

necessary, multi-unit fabrication can begin. This involves keeping a supply of known good components and package elements while further units are produced and tested. During this production stage, additional modifications or enhancements to the system software can take place. Although the map is specific to the development of the μCluster, it is consistent with the work that will be necessary in similar microsystem projects.

10.7.2 Packaging

Three areas of packaging were investigated: sensor packaging, multichip packaging, and external system packaging. In sensor packaging, one fundamental question is whether to fabricate the sensors as hybrid devices with separate die for the transducer and the readout/interface electronics or whether to make them monolithic, all on the same integrated circuit die. Advantages of a hybrid design are higher yield (two chips can be fabricated and tested individually), independent iteration of the design of each chip, and reduced process complexity. Advantages of a monolithic design are reduced interconnect requirements and improved performance by having the readout circuit on the same chip as the transducer. In general, hybrid designs make system-level development more difficult; while monolithic designs make component-level development more difficult. In most cases, performance will be better with monolithic devices. However, for the initial μCluster, a hybrid design allowed designers of the state-of-the-art transducers the freedom to work without the encumbrance of interface circuitry.

A most important area in sensors today is monolithic packaging technology used to build the first-level package directly on the chip with the transducers. These packages use deposited thin films such as silicon dioxide and silicon nitride, possibly with metal barriers against moisture and chemical contaminants from the environment. In some implantable sensors for biomedical applications, these films are the only package possible.[70] As the technology is further developed, silicon carbide and diamond films may be used for chip-level packaging as well. In addition, chemical vapor deposition (CVD),[71] silicon-glass anodic bonding,[72] and silicon-silicon fusion bonding[52] are used to form wafer-level vacuum cavities for devices such as accelerometers, where the variable can be coupled through a hermetically sealed microstructure.

For hybrid devices, sensor packaging remains an important issue. At this level, the sensor package is a surface on which the hybrid sensors and interface components are mounted and connected using flip-chip or wire bond techniques. Packaging also consists of sealing the chips and placing them in an outer shell to protect against the environment (moisture, dust, radiation, etc.). This multichip-module (MCM) approach minimizes the size of the overall system by eliminating intermediate chip packaging and brings the components together as closely as possible on a common substrate. The approach also allows different technologies to be used as needed (e.g., monolithic sensors, silicon-on-glass hybrids, or silicon-silicon fusion-bonded structures). The package technology chosen for a given microsystem depends on the application and may also depend on the number of units to be produced. In the case of the μCluster, the packaging options were limited by the available in-house equipment. A multilayer printed circuit board (PCB) was chosen as the substrate for the μCluster since it allowed components to be easily attached and connected either by wire bonding or soldering. This approach was also good for prototype development because the board could be altered much more easily than in some other MCM technologies that bury components deep within the package.

The PCB for the μCluster was designed such that all the components, including the sensors, the wireless transmitter, and a 10-pin hardwired I/O connector, are attached on the top of the board. This gave easy access to test points on the board and simplified the replacement of components. Figure 10.21 shows a populated μCluster PCB with the components labeled. Contact

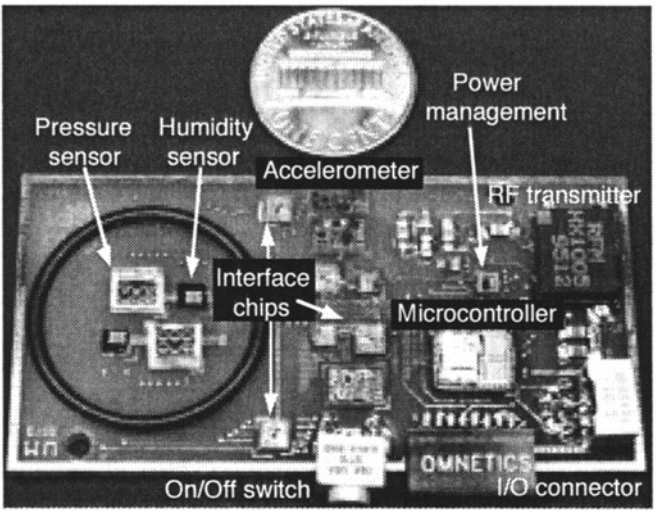

Fig. 10.21. A populated μCluster PCB showing the layout of the components on the system.

points for two 3-V coin-cell batteries are on the back of the board. Because some of the sensors on the μCluster require access to the environment that they monitor, the entire μCluster could not be sealed in an external package, and yet most of the electronics should be sealed from environmental effects. To accommodate these conflicting needs, the package designed for the μCluster includes an O-ring that is sealed to the PCB. The O-ring works with the external package to isolate the sensing elements that need environmental access from the rest of the system. A port on the external package has an open path between the area within the O-ring and the outside environment. The rest of the system is sealed from the outside environment by the external package, which for the μCluster is an anodized aluminum case. This material can easily be machined to the desired form and provides good electrical isolation. The antenna for the wireless transmitter passes through and wraps around the external package. A wrist strap can be attached to the package so that the μCluster can we worn in wrist-watch fashion as shown in Fig. 10.22.

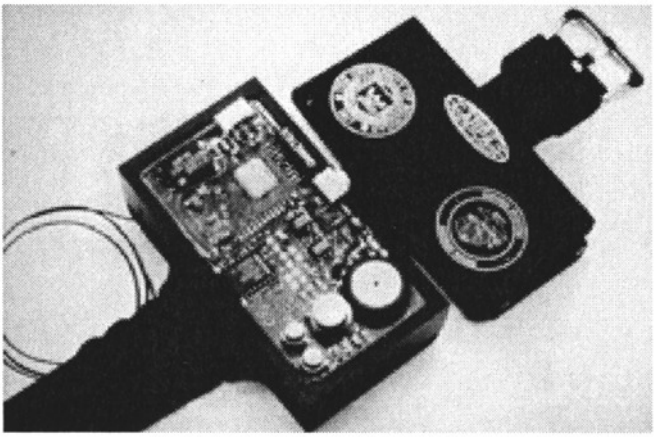

Fig. 10.22. A packaged μCluster in an anodized aluminum case with a wrist strap, which makes the system a wearable unit.

10.7.3 Testing

During development of the μCluster a number of testing steps were identified to provide final sensor calibration and system specification. The first-level tests were to find known good die for the components used on the μCluster. Commercial components have usually already undergone this type of test, but all custom components had to be tested after fabrication so that only components known to work within specifications would populate the system. After these tests, the system could be populated and checked for basic functionality. The following series of preliminary tests was run to ensure all the components were operating and communicating as expected.

- External communication with the MCU
- Read and write of the MCU memory
- Communication between the MCU and the power management chip
- Power management functions (power switching, sleep mode, etc.)
- Communication between the MCU and the sensor interface chip(s)
- Wireless transmission of test data

After these preliminary tests, the μCluster must undergo a variety of tests designed to calibrate and compensate each of the sensors on the system. Here we will define calibration as setting the electrical output of the sensor to the appropriate level over the desired range of measurement, that is, adjusting gains and offsets, and then compensating to remove cross-parameter (temperature) sensitivities. To calibrate each sensor, tests were first run to determine the appropriate gain and offset adjustments in the capacitive sensor interface chip (CSIC). To tune the response more finely, the CSIC could then be laser-trimmed to provide the maximum sensitivity for each sensor. If any trouble with either the transducer or the CSIC was found at this time, the component could be removed and replaced. After these initial sensor tests, a protective coating had to be placed over the wire bonds connecting the sensor to its readout chip in order to protect it from environmental effects such as humidity. Unfortunately, this coating would often cause a shift in sensor output by altering the parasitic capacitance associated with the transducer inputs, necessitating additional final adjustments that must be made electronically. Similar system-level tests were then performed to ensure no problems occurred during the packaging process. After this, the system was tested to measure parameters such as power consumption (and battery life), wireless transmission range, and sensor performance over an environmental temperature range (−20°C to +50°C). The results of such tests are given below.

10.7.4 Calibration and Compensation

One of the primary goals of this particular microsystem was to demonstrate a fully calibrated sensing system capable of delivering data to a host system that required no further data processing. This feature frees the host system to do higher-level operations. To accomplish this goal the μCluster uses a combination of hardware and software techniques. The hardware techniques have been discussed and involve electronic and laser trimming of the sensor readout circuitry to set the gain and offset of the switched capacitor circuit. However, these techniques are of limited use since they only provide coarse adjustments, do not sufficiently address nonlinear effects, and do not correct for undesired temperature sensitivities. Digital compensation, where the data corrections are performed in software, offers the ability to perform all these adjustments and can result in an order-of-magnitude improvement in device accuracy.[73]

Three traditional methods of implementing digital compensation are look-up tables, polynomial computation, and some combination of the two. Choice of approaches is largely determined by the degree of linearity displayed by the sensor, the required accuracy, and the time it takes to

complete the digital calibration task. (This last issue is of special importance in low-power systems such as the μCluster.) There are highly developed design-of-experiments procedures that allow the number of test points to be minimized and positioned for a given degree of accuracy.[74]

Except for the temperature sensor, which uses a combination method, the sensors on the μCluster employ polynomial compensation techniques. The accelerometer uses the most basic form of polynomial because it has a highly linear response. Therefore, a simple $y = mx + b$ equation can be applied, where x is the measured sensor output, m and b are coefficients determined by testing each accelerometer, and y is the resulting acceleration. By storing values for m and b in the memory of the MCU, the proper acceleration level can be obtained with a simple two-step mathematical operation on the measured data. Calibration of the accelerometer is further simplified because it does not display a significant temperature dependence over the desired operating range and can, therefore, be calibrated by a one-variable equation.

The other sensor on the μCluster that can be calibrated by a one-variable equation is the temperature sensor; however, this sensor is highly nonlinear, with an output response that fits a logarithmic curve, making calibration much more complex. If polynomial compensation is used, a 5th-order equation is necessary to obtain the desired accuracy from this sensor. At a minimum, evaluating the 5th-order equation requires nine multiplications and five additions and uses six coefficients. This can require significant MCU processing time, reducing system bandwidth and increasing power consumption. An alternative approach, taken with the temperature sensor, is to break the sensor output into multiple segments and then fit a lower-order polynomial to each segment. With this method the MCU need only compare the measured data to a set of segment values to determine which segment equation to use. For this sensor a 2nd-order polynomial in each of four 20°C segments was as accurate as a 5th-order polynomial over the entire range, yet required only three multiplications, two additions, and 12 coefficients. Another scheme, shown in Fig. 10.23, uses linear equations over each of eight 10°C segments requiring 1 multiplication, 1 addition, and 16 coefficients for the same accuracy. Note in Fig. 10.22 that the lines form a logarithmic curve as should be expected. Similar methods could be used by many transducers, but the chosen method must match the needs of the system and the specific sensor.

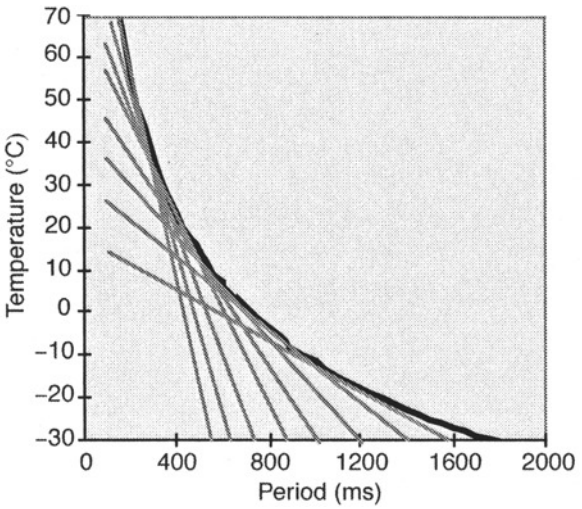

Fig. 10.23. Temperature sensor output as it is fit by linear equations each covering a 10°C segment. The actual response of the sensor is shown by the darker line.[65]

The calibration method used on the μCluster pressure and humidity sensors is a two-variable 4th-order polynomial that has been fit to a set of data taken over temperature and the sensed parameter (pressure, humidity). This equation has 25 terms to be evaluated and summed in calculating the true output. However, many of these terms have negligible effect on the calculation and can be ignored, reducing the equation to about 10 to 15 significant terms. The advantage of this digital calibration approach is that even a very nonlinear sensor response can be accurately tracked across the measurement range. Figure 10.24 shows an example of a pressure sensor output as a function of pressure and temperature that is tracked very well by the 4th-order compensation polynomial.

10.7.5 Final Results

Table 10.6 summarizes the characteristics of the University of Michigan Microinstrumentation Cluster. This multiparameter sensing microsystem can be seen in Figs. 10.21 and 10.22. To provide feedback regarding the design and operation of the μCluster, several units have been assembled, calibrated, and packaged. These units are either in use or available for use by other research agencies where field trials and experiments are being conducted to evaluate the performance of the μCluster. μCluster units at the Naval Research Laboratory (Washington, D.C.) are being flown on unmanned air vehicles. Units have also been delivered to researchers at the Naval Command, Control, and Ocean Surveillance Center, where they will be deployed on ocean buoys to measure environmental parameters. Previously, μCluster units have been taken on field exercises with the U.S. Marine Corps (Fig. 10.25). Here field trials were conducted to evaluate the μCluster's ability to provide meteorological data used for calculations on the trajectories of artillery fire.

Ongoing research efforts seek to improve the performance of both the microsystem and the integrated sensors employed on the system. Additionally, a variety of new sensors are being investigated for use in future microsystems. These new microsensors will be compatible with the low-power and small-size goals of the μCluster while adding the ability to monitor acoustic and

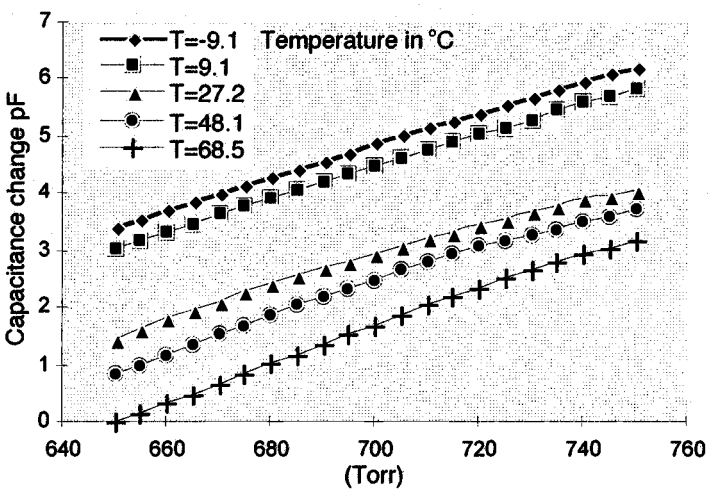

Fig. 10.24. Barometric pressure sensor output at various temperatures.[60] Note that the nonlinearity of the response that can be accurately tracked with a two-variable 4th-order calibration polynomial that also compensates the sensor's sensitivity to temperature.

chemical phenomena, as well as providing additional navigational data (acceleration and rate of turn). The future of microsystems in the world of electronics is indeed bright, and the intelligent operation of the μCluster is just the beginning of what the MEMS industry will provide in the years to come.

Table 10.6. Specifications for the Microinstrumentation Cluster

Configuration	Wristwatch/Business Card
Internal system volume	5/15 cc
Power supply	External 6-V/275-mA-hr coin cell batteries Standard 9-V batteries
Telemetry range	>100 ft
Telemetry frequency / modulation	315 MHz/ASK
Average power dissipation[a]	<500 μW
Portable operating life[a]	90 days
Measurement aperture time	10 μsec
Minimum scan interval	60 μsec
Sensor scan rate	1/minute (typical) adaptive and event-triggered

[a]Operating mode dependent

Fig. 10.25. U.S. marine wearing a μCluster during Operation Steel Knight V. Notice that the unit can be strapped to the soldier's wrist while it transmits data to a remote receiver and laptop PC.

10.8 Appendixes

Appendix 10.A COTS Micro/Nano Accelerometers

Model	FS Input (+-G)	FS Output (V)	Band-width (Hz)	Max Rating (g)	Noise (g)	PS (V)	Current (ma)	Size/Wt (in.,in.,in./gm)
				Analog Devices				
ADXL05	0.05	0.8–2.8	4000	500–1000	0.032	4.75–5.25	8	10 pin TO-100/5
ADXL50	50	0.8–2.8	4000	500–2000	0.4	4.75–5.25	10	10pin TO-100/5
ADXL151	50	3.8	1000	500–1000	0.03	4–6	1.8	0.49,0.10, 0.21/5.0
ADXL250 two axis	50	3.8	1000	500–1000	0.03	4–6	3.5	0.49,0.10, 0.21/5.0
				IC Sensors				
3255-050	50	0.5–4.5	0–2000	2000	0.25	4.5–7	10	0.53,0.30,0.16/1.5
3255-250	250	0.5–4.5	0–3000	2000	1.3	4.5–7	10	0.53,0.30,0.16/1.5
3255-500	500	0.5–4.5	0-3000	200	2.5	4.5–7	10	0.53,0.30,0.16/1.5
3140-002	2	0.5–4.5	0–250	40	0.005	8–30	5	0.9,0.6,0.21/6.5
3140-005	5	0.5–4.5	0–500	100	0.0013	8–30	5	0.9,0.6,0.21/6.5
3140-010	10	0.5–4.5	0–700	2000	0.0025	8–30	5	0.9,0.6,0.21/6.5
3140-020	20	0.5–4.5	0–1050	4000	0.005	8–30	5	0.9,0.6,0.21/6.5
3140-050	50	0.5–4.5	0–1600	10000	0.013	8–30	5	0.9,0.6,0.21/6.5
3140-100	100	0.5–4.5	0–2300	20000	0.025	8–30	5	0.9,0.6,0.21/6.5
3140-200	200	0.5–4.5	0–2500	4000	0.05	8–30	5	0.9,0.6,0.21/6.5
3022-002-p	2	-0.03–0.03	0–250	400	0.00007	5	1.5	0.9,0.6,0.21/6.5
3022-005-p	5	-0.55–0.055	0–300	400	8.00E-05	5	1.5	0.9,0.6,0.21/6.5
3022-010-p	10	-0.45–0.45	0–400	400	0.00022	5	1.5	0.9,0.6,0.21/6.5
3022-020-p	20	-0.045–0.045	0–600	400	0.00044	5	1.5	0.9,0.6,0.21/6.5
3022-050-p	50	-0.55–0.055	0–1000	1000	0.0008	5	1.5	0.9,0.6,0.21/6.5
3022-100-p	100	-0.45–0.45	0–1500	2000	0.0022	5	1.5	0.9,0.6,0.21/6.5
3022-200-p	200	-0.045–0.045	0–2000	2000	0.0044	5	1.5	0.9,0.6,0.21/6.5
3022-500-p	500	-0.55–0.055	0–2400	2000	0.008	5	1.5	0.9,0.6,0.21/6.5
3355-025 Triaxial	25	0.5–4.5	0–1000	2000	0.13	4.5–7	10	1.25,1.25,0.575/35

Appendix 10.A COTS Micro/Nano Accelerometers—*Continued*

Model	FS Input (+-G)	FS Output (V)	Band-width (Hz)	Max Rating (g)	Noise (g)	PS (V)	Current (ma)	Size/Wt (in.,in.,in./gm)
3355-050 Triaxial	50	0.5–4.5	0–2000	2000	0.025	4.5–7	10	1.25,1.25,0.575/35
3355-100 Triaxial	100	0.5–4.5	0–3000	2000	0.5	4.5–7	10	1.25,1.25,0.575/35
3355-250 Triaxial	250	0.5–4.5	0–3000	2000	1.3	4.5–7	10	1.25,1.25,0.575/35
				Kistler				
8302B2S1	2	0–5	0–300	2000	2.5E-05	12–36	40	0.7,0.625,0.2/2.8
8302B10S1	10	0–5	0–180	2000	0.00013	12–36	40	0.7,0.625,0.2/2.8
8302B20S1	20	0–5	0–160	2000	0.00025	12–36	40	0.7,0.625,0.2/2.8
				Silicon Design				
1210x-010	10	0.5–4.5	0–800	2000	0.002	4.75–5.25	2	0.35,0.35,0.105/.75
1210x-025	25	0.5–4.5	0–1000	2000	0.005	4.75–5.25	2	0.35,0.35,0.105/.75
1210x-505	50	0.5–4.5	0–1600	2000	0.01	4.75–5.25	2	0.35,0.35,0.105/.75
1210x-100	100	0.5–4.5	0–2000	2000	0.02	4.75–5.25	2	0.35,0.35,0.105/.75
2210-10	10	0.5–4.5	0–800	2000	0.002	9–30	9	1.2,1.2,1/16
2210-25	25	0.5–4.5	0–1000	2000	0.005	9–30	9	1.2,1.2,1/16
2210-50	50	0.5–4.5	0–1600	2000	0.01	9–30	9	1.2,1.2,1/16
2210-100	100	0.5–4.5	0–2000	2000	0.02	9–30	9	1.2,1.2,1/16
2412-50 Triaxial	1210	0.5–4.5	see 1210	2000	see 1210	4.75–5.25	6	1.2,1.2,1/16
				Endevco				
7290A-10	10	-2 – +2	500	5000–40	0.01	9.5–18	7.5	1,0.83,0.30/10
7290A-30	30	-2 – +2	800	5000–40	0.01	9.5–18	7.5	1,0.83,0.30/10
7290A-100	100	-2 – +2	1000	5000–40	0.01	9.5–18	7.5	1,0.83,0.30/10
7264-200	200	-0.5 – +5	0–1000	1000	6	10–15	3.6	0.4,0.3,0.2/1
7264-2000	2000	-0.5 – +.5	0–5000	1000–10000	60	10–15	3.6	0.4,0.3,0.2/1
7265A	100	-0.5 – +5	800	1000	2	10–15	1.4	0.63,0.47,0.3/6
7265A/A-HS	20	-0.5 – +5	500	1000	2	10–15	1.4	0.63,0.47,0.3/6

Appendix 10.A COTS Micro/Nano Accelerometers—*Continued*

Model	FS Input (+-G)	FS Output (V)	Band-width (Hz)	Max Rating (g)	Noise (g)	PS (V)	Current (ma)	Size/Wt (in.,in.,in./gm)
7265AM3	2000	-0.5 – +.5	0–4000	1000–5000	40	10–15	1.4	0.63,0.47,0.3/6
7267A Triaxial	1500	-0.225–0.225	1200 – 2000	1000	3	10–15	0.1	0.9,0.75,0.75/50
				Silicon Microstructures				
SM-7130-010	10	1.5–3.5	0–500	2000	0.05	9–20	6	1.4,0.8 ,0.32/6
SM-7130-050	50	1.5–3.5	0–800	2000	0.2	9–20	6	1.4,0.8 ,0.32/6
SM-7130-100	100	1.5–3.5	0–2000	2000	0.5	9–20	6	1.4,0.8 ,0.32/6
SM-7130-300	300	1.5–3.5	0–2000	2000	1.5	9–20	6	1.4,0.8 ,0.32/6
				Entran Devices				
EGA-125F-10D	10	NA	250	50	0.1	15	NA	0.27,0.14,0.14/0.5
EGA-125F-25D	25	NA	500	125	0.25	15	NA	0.27,0.14,0.14/0.5
EGA-125F-100D	100	NA	750	500	1	15	NA	0.27,0.14,0.14/0.5
EGA-125F-250D	250	NA	1000	3000	2.5	15	NA	0.27,0.14,0.14/0.5
EGA3 Triax range	NA	NA	NA	NA	NA	NA	NA	0.5,0.5,0.5/3
EGE-73B2-200F	200	NA	500	2000	4	pos/neg 10	13	0.48,0.4,0.18/1
EGE-73B2-100D	100	NA	800	2000	1	pos/neg 10	13	0.48,0.4,0.18/1

Appendix 10.B Survey of Microcontrollers/Data Loggers

Attribute	PC 104[a]	Tattle-Tale 8 Card[b]	MicroChip PIC Controller[c]	Apple Newton[d]
CPU/memory	486 DX /16 Mbytes RAM; 4Mbytes Flash ROM	M68332 & PIC16C64/ 256kbytes RAM; 256 kbytes Flash /2k EEPROM	PIC17C756/32 kB Flash, 900 B RAM	StrongARM, 160 MHz/32 Mbytes
ADC at sample rate (kHz), 12-bit accuracy	8 inputs at 100[e]	8 inputs at 100	10 inputs at[f]	8 inputs at 100[e]
No. of DACs, 10-bit accuracy	NA[g]	NA[g]	NA[g]	none
No. digital I/O lines	[h]	14	50	NA[g]
Serial Ports at bps	2 ports[e]	2 ports at 500 kbps max	2	1 port at 150
Power (W)	10 at 66 MHz	0.30 at 20 MHz	0.20 at 33 MHz	0.45 at 160 MHz
Voltage levels (V)	5,12	7–15	2.5–6.0	3.3
Low-power capability, power (mW)	Yes, 1.3	Yes, 1	Yes, 0.05	Yes, 0.15
Internal clock rate (MHz)	100	Adj to20 max	Adj to 33	160
Environmental:				
Temp. range (°C)	0–50	0–70	Commercial/industrial	0–45
Acceleration	20 G	[f]	NA[g]	NA[g]
Radiation tolerant	no	no	no	no
Weight (g)/size (mm)	[f]/96×90×23	28/5×76×13	<1/12×12×1.2	985/250×114×64
Language supported	NA[g]	ANSI C or TxBasic	C or 58 RISC Instruction Set	ANSI C
Space experience	[f]	Data Loggers used in Shuttle space suits	MightlySat	None
Website	http://www.controller.com/pc104	http://www.onsetcomp.com	http://www.microchip2.com	NA[g]
Design standard	IEEE P996.1	NA[g]	NA[g]	NA[g]

[a]S-MOS System, Inc, San Jose, CA.
[b]Onset Computers, Pocasset, MA.
[c]Microchip Technology, Chandler, AZ.
[d]Digital Electronics produces ARM(Advanced RISC Machines) chips under license.
[e]With PCMCIA card.
[f]Unknown
[g]Not applicable
[h]Available as add-on modules from PC/104 consortium members such as WinSystems, Arlington, TX; Ampro Computers, Sunnyvale, CA; Micro/Sys, Inc, Glendale, CA; and similar sources.

Appendix 10.C Survey of Microcontrollers/Data Loggers

Attribute	Honeywell Time Stamp Measurement Device (TSMD)[a]	University of Michigan Microcluster Watch	Adcon Telemetry m-T	Phillips Lab Advanced Instrumentation Controller
CPU/Memory	87C51/128 kbytes RAM; 32 kbytes EEPROM; 256 bytes Ser. RAM	MC68HC11/768 bytes RAM,24 kbytes ROM or EPROM.640 bytes EEPROM	MC68HG11/ 12kbytes ROM, 512 bytes EEPROM.2-32Ser. EEPROM	8051/128 kbytes SRAM128 kbytes nonvolatile
ADC at sample rate (kHz)/ bit accuracy	7 at [b]/8	8 at 125/8	4 at 125/8	32 inputs MUXed at 25
No of DACs,10-bit accuracy	0	0	0	8
Serial Ports at kbps	1 port at 96	1 port at19 or 31	1 port at 19 or 31	6 ports
Power(W)	0.10	0.22	0.35	0.050 at 1 MHz
Voltage levels(v)	5	6	5-7	5, 3.3
Low-power capability, power, mW	Yes, [b]	Yes. 0.075	Yes, 0.5	Yes, 0.5
Internal clock rate(MHz)	0.3 & 11	Adj to 4	5	10
Environmental				
Temp range(oC)	-55 to 125	-40 to 125	[b]	Room to 120
Acceleration	15 kGs			30 kGs
Radiation tolerant	Yes			
Size(mm)	25 × 51 × 5	14 × 14 × [b]	70 × 29 × 8	3/25 × 40 × 2
Space Experience				Designed for Mission to Mars

[a]See Ref. 73.
[b]Unknown

10.9 References

1. J. Hosticka, "CMOS Sensor Systems," *Digest, Int. Conf. on Solid-State Sensors and Actuators (Transducers '97)*, (Chicago, June 1997), pp. 991–993.
2. J. Bryzek, "MEMS: A Closer Look," *Sensors Magazine*, July 1996, 4–9.
3. H. Huijsing, F. R. Riedijk, and G. van der Horn, "Developments in Integrated Smart Sensors," *Digest, Int. Conf. on Solid-State Sensors and Actuators (Transducers '93)*, (Yokohama, Japan, June 1993), pp. 320–326.
4. K. D. Wise, "Microelectromechanical Systems: Interfacing Electronics to a Non-Electronic World," *Digest, IEEE Int. Electron Device Meeting*, pp. 11–18, December 1996.

5. L. Spangler and C. J. Kemp, "A Smart Automotive Accelerometer with On-Chip Airbag Deployment Circuits," *Digest, Solid-State Sensor and Actuator Workshop* (Hilton Head Island, SC, June 1996), pp. 211–214.
6. H. Baltes, H. Haberli, P. Malcovati, F. Maloberti, "Smart Sensor Interfaces," *Digest, IEEE Int. Symposium on Circ. and Systems* (Atlanta GA, May 1996), vol. 4, pp. 380–383.
7. E. Yoon, K. D. Wise, "An Integrated Mass Flow Sensor with On-Chip CMOS Interface Circuitry," *IEEE Trans. Electron Devices* 39 (6), 1376–1386 (1992).
8. M. Clarkson, "Smart Sensors," *Sensors Magazine*, May 1997, 14–20.
9. K. D. Wise, "Integrated Microinstrumentation Systems: Smart Peripherals for Distributed Sensing and Control, Digest, *IEEE Int. Solid-State Circ. Conf.* (San Francisco, February 1993), pp. 126–127.
10. S. Middlehoek and S. A. Audet, *Silicon Sensors* (Academic Press, London, 1989).
11. E. S. Robinson, "ASIM Application in Current and Future Space Systems," in *Microengineering Technology for Space Systems*, edited by H. Helvajian, Monograph 97-02 (The Aerospace Press, El Segundo, CA, 1997). First published as The Aerospace Corp. Report no. ATR-95(8168)-2 (1995).
12. I. Chang, "Investigation of Space Related Mission Failures," The Aerospace Corp. Report no. TOR-94(3530)-04 (1994).
13. S. Amimoto, "Multiparameter Sensor for Launch Vehicle Application," Briefings to the Air Force Space and Missile Systems Center Chief Engineering Office on MEMS Application to Space Systems, El Segundo, CA, May 1995 (unpublished).
14. "Delta Explosion Halts $1 Billion in Launches," *Aviation Week and Space Technology*, 27 Jan. 1997.
15. E. E. Kalmi, WIS 44/K11 Configuration Document, Martin Marietta, 17 May 1993, and M. Becker, Titan IV PCM Measurement List, Lockheed-Martin, Contract no. F04701-96-C-001 (30 Aug. 1996).
16. E. Moss, "Engineering Test Order for LOIS," Martin Marietta Report no. TIV-89-34 (27 March 1990).
17. G. N. Smit, "Performance Threshold for Application of MEMS Inertial Sensors in Space," *Microengineering Technology for Space Systems*, edited by H. Helvajian, Monograph 97-02 (The Aerospace Press, El Segundo, CA, 1997). First published as The Aerospace Corp. Report no. ATR-95(8168)-2 (1995).
18. E. E. Kalmi, Martin Marietta WIS 44/K11 Configuration Document (17 May 1993); M. Becker, "Titan IV PCM Measurement List," Lockheed-Martin Contract no. F04701-96-C-001. (30 Aug. 1996); and E. Moss, "Engineering Test Order for Lift-Off Instrumentation System," Martin Marietta Report no. TIV-89-34 (27 March 1990).
19. K. Feher, *Wireless Digital Communication* (Prentice Hall PTR, Upper Saddle River, NJ, 1995).
20. A. Zatsman, *et al.*, "Industry's First Integrated Wavelet Video Codec Sets New Standards for Cost, Image Quality and Flexibility," *Analog Dialog* 30-2, 7–9 (1996).
21. J. C. Lykes, "Packaging Technologies for Space-Related Microsystems and Their Elements," in *Microengineering Technology for Space Systems*, edited by H. Helvajian, Monograph 97-02 (The Aerospace Press, El Segundo, CA, 1997). First published as The Aerospace Corp. Report no. ATR-95(8168)-2 (1995).
22. P. Madan, "Infranets, Intranets, and the Internet," *Sensors* 14 (3), 46–50 (1997).
23. J. Warrier, "Smart Sensor Networks of the Future," *Sensors* 14 (3), 40–45 (1997).
24. R. Bernstein, "The LONWORKS Standard," Echelon Product Seminar, Marina del Rey, 31 March 1997. See also Wide World Web sites for Echelon <http://www.echelon.com> and for LonMark: <http://www.lonmark.org>.
25. J. Kuhnel, "Voltage Regulators for Power Management," *Analog Dialog* 30-4, 13–15 (1996).
26. M. Robyn, L. Thaller, and D. Scott, "Nanosat Power System Considerations," in *Microengineering Technology for Space Systems*, edited by H. Helvajian, Monograph 97-02 (The Aerospace Press, El Segundo, CA, 1997). First published as The Aerospace Corp. Report no. ATR-95(8168)-2 (1995).
27. B. Schweber, "Choices and Confusion Spread Wider as Spread Spectrum Goes Mainstream," *EDN* (European edition) 41 (21), 79–87 (10 October 1996).
28. K. Feher, *Wireless Digital Communication*, p. 269.

29. W.H. Hsieh, T.Y. Hsu, and Y. C.Tai, "A Micromachined Thin-film Electret Microphone," paper 2B2b02, and M. Pedersen, W. Oulthuis, and P. Bergveld, "A Polymer Condenser Microphone on Silicon with On-ship CMOS Amplifier," paper 2B2.07, *1997 Int. Conf. on Solid-State Sensors and Actuators (Transducers'97)*, (Chicago, IL, June 1997) pp. 6–19.
30. Rubic Sarian, Harris Semiconductor, Nov. 1997, private communication.
31. W. L. Pritchard and J. A. Sciulli, *Satellite Communications Systems Engineering* (Prentice Hall, Inc., Inglewood Cliffs, NJ, 1986) p. 170.
32. S. T. Amimoto, R. Crespo, E. W. Fournier, J. V. Osborn, H. Ozisik, B. H. Weiller, E. M. Yohnsee, "Development of Launch Vehicle Nanotechnology Instrumentation at The Aerospace Corporation," *Proceedings of the 44th International Instrumentation Symposium* (Reno, NV, 3–7 May 1998), pp. 240–248.
33. K. Bult, A. Burstein, D. Chang, M. Dong, M. Fielding, E. Kruglick, J. Ho, F. Lin, W. J. Kaiser, H. Marcy, R. Mukai, P. Nelson, F. Newberg, K.S.J. Pister, G. Pottie, H. Sanchez, O. M. Stafsudd, K. B. Tan, C. M. Ward, S. Xue, and J. Yao, "Low Power Systems for Wireless Microsensor," *1996 International symposium on Low Power Electronics and Design, Digest of Technical Papers*, pp. 17–21; and W. J. Kaiser, "Low Power Wireless Integrated Microsensors LWIM)," *MEMS DARPA PI Meeting* (July 1998).
34. A. Mason, N. Yazdi, K. Najafi, K. D. Wise, "A Low-Power Wireless Microinstrumentation System for Environmental Monitoring," *Digest Int. Conf. on Solid-State Sensors and Actuators* (Stockholm, June 1995), pp. 107–110.
35. K. D. Wise, "Integrated Microinstrumentation Systems: Smart Peripherals for Distributed Sensing and Control," *Digest 1993 IEEE Int. Solid-State Circuits Conf.* (San Francisco, February 1993), pp. 126–127.
36. K. D. Wise, "Microelectromechanical Systems: Interfacing Electronics to a Non-Electronic World," (invited plenary), *Technical Digest, Int. Electron Devices Meeting* (San Francisco, December 1996), pp. 11–18.
37. Samaun, K. D. Wise, and J. B. Angell, "An IC Piezoresistive Pressure Sensor for Biomedical Instrumentation," *Int. Solid-St. Circuits Conf. Digest of Tech. Papers* (February 1971), pp. 104–105.
38. S. Sugiyama, M. Takigawa, and I. Igarashi, "Integrated Piezoresistive Pressure Sensor with both Voltage and Frequency Output," *Sensors and Actuators* 4, 113–120 (September 1983).
39. W. Yun, R. T. Howe, and P. R. Gray, "Surface Micromachined Digitally Force-Balanced Accelerometer with Integrated CMOS Detection Circuitry," *Digest IEEE Solid-State Sensor and Actuator Workshop* (Hilton Head, SC., June 1992), pp. 126–129.
40. T. Ohnstein, *et. al*, "Environmentally Rugged Wide Dynamic Range Microstructure Airflow Sensor," *Digest IEEE Solid-State Sensor and Actuator Workshop*, Hilton Head, SC. (1990), 158–160.
41. J. Bernstein, *et al.*, "A Micromachined Comb-Drive Tuning Fork Rate Gyroscope," *Proc., IEEE Microelectro-mechanical Systems Workshop* (February 1993), pp. 143–148.
42. M. W. Putty and K. Najafi, "A Micromachined Vibrating Ring Gyroscope," *Digest Solid-State Sensor and Actuator Workshop* (Hilton Head, June 1994), pp. 213–220.
43. I. H. Choi and K. D. Wise, "A Silicon Thermopile-Based Infrared Sensing Array for use in Automated Manufacturing," *IEEE Trans. Electron Devices* 33, 72–79 (January 1986).
44. R. A. Wood, C. J. Han, and P. W. Kruse, "Integrated Uncooled Infrared Detector Imaging Arrays," *Digest IEEE Solid-State Sensor and Actuator Workshop* (June 1992), pp. 132–135.
45. W. C. Tang, T.-C. H. Nguyen, and R.T. Howe, "Laterally Driven Polysilicon Resonant Microstructures," *Sensors and Actuators* 20, 25–32 (1989).
46. R. S. Payne and K. A. Dinsmore, "Surface Micromachined Accelerometer: A Technology Update," Digest SAE Meeting, Detroit, pp. 127–135, February 1991.
47. C. T.-C. Nguyen and R. T. Howe, "Quality-Factor Control for Micromechanical Resonators," *Digest Int. Electron Devices Meeting* (December 1992) pp. 505–508.

48. J. B. Sampsell, "The Digital Micromirror Device and Its Application to Projection Display," *Digest of Technical Papers 7th Int. Conf. on Solid-State Sensors and Actuators (Transducers '93)*, (IEE of Japan, 1993), pp. 24–27.
49. P. L. Bergstrom, J. Ji, Y. Liu, M. Kaviany, and K. D. Wise, "Thermally Driven Phase-Change Actuation," *IEEE J. of Microelectromechanical Systems* 4, 10–17 (March 1995).
50. H. Seidel, L. Csepregi, A. Heuberger, and H. Baumgartel, "Anisotropic Etching of Crystalline Silicon in Alkaline Solutions," *J. Electrochem. Soc.*, 3612–3632 (November 1990).
51. W.-H. Juan and S. W. Pang, "Released Si Microstructures Fabricated by Deep Etching and Shallow Diffusion," *IEEE J. Microelectromechanical Systems* 5, 18–23 (March 1996).
52. M. A. Schmidt, "Silicon Wafer Bonding for Micromechanical Devices," *Digest Solid-State Sensor and Actuator Workshop* (Hilton Head, SC., June 1994), pp.127–131.
53. H. Guckel, T.R. Christenson, K.J. Skrobis, J. Klein, and M. Karnowsky, "Design and Testing of Planar Magnetic Micromotors Fabricated by Deep X-Ray Lithography and Electroplating," *Digest 7th Int. Conf. on Solid-State Sensors and Actuators (Transducers '93)*, (IEE of Japan, 1993), pp. 76–79.
54. R. T. Howe, "Surface Micromachining for Microsensors and Microactuators," *J. of Vacuum Science and Technology, B* 6, 1809–1813 (December 1988).
55. H. Guckel and D. W. Burns, "Planar Processed Polysilicon Sealed Cavities for Pressure Transducer Arrays," *Digest IEEE IEDM* (December 1984).
56. C. H. Mastrangelo and C. H. Hsu, "Mechanical Stability and Adhesion of Microstructures under Capillary Forces," *IEEE J. Microelectromechanical Systems* 2, 33–62 (March 1993).
57. Y. Zhang and K. D. Wise, "A High-Accuracy Multi-Element Silicon Barometric Pressure Sensor," *Digest Int. Conf. on Solid-State Sensors and Actuators* (Stockholm, June 1995), pp. 608–611.
58. S. T. Cho and K. D. Wise, "A High-Performance Microflowmeter with Built-In Self-Test," *Sensors and Actuators, A*, 47–56 (March 1993).
59. N. Yazdi, A. Mason, K. Najafi, K. Wise, "A Low-Power Generic Interface Circuit for Capacitive Sensors", *Digest, Solid-State Sensor and Actuator Workshop* (Hilton Head Island, SC, June 1996), pp. 215–218.
60. A. Chavan and K. D. Wise, "A Batch-Processed Vacuum-Sealed Capacitive Pressure Sensor," *Digest IEEE Int. Conf. on Solid-State Sensors and Actuators* (Chicago, June 1997), pp. 1449–1452.
61. W. G. Baer, K. Naafi, K. D. Wise, and R. S. Toth, "A 32-Element Micromachined Thermal Imager with On-Chip Multiplexing," *Sensors and Actuators, A: Physical* 48 (1), 47–54 (1 May 1995).
62. C. C. Liu and C. H. Mastrangelo, "An Ultrasensitive Uncooled Heat-Balancing Infrared Detector," *Digest IEEE Int. Electron Devices Meeting* (December 1996), pp. 549–552.
63. N. Najafi, K. D. Wise, and J. W. Schwank, "A Micromachined Ultra-Thin-Film Gas Detector," *IEEE Trans. Electron Devices* 41,1770–1777 (October 1994).
64. S. Majoo, J. W. Schwank, J. L. Gland, and K. D. Wise, "A Selected-Area CVD Method for Deposition of Sensing Films on a Monolithic Integrated Gas Detectors," *IEEE Electron Device Letters*, pp. 217–219 (May 1994).
65. A. Mason, N. Yazdi, A. V. Chavan, K. Najafi, K. D. Wise, "A Generic Multielement Microsystem for Portable Wireless Applications," *Proceedings of the IEEE* 6 (8), 1733–1746 (August 1998).
66. S. C. Terry, J. H. Jerman, and J. B. Angell, "A Gas Chromatographic Air Analyzer Fabricated on a Silicon Wafer," *IEEE Trans. Electron Devices* 26,1880–1886 (December 1979).
67. N. Najafi, K. D. Wise, "An Organization and Interface for Sensor-Driven Semiconductor Process Control Systems," *IEEE Tran. on Semiconductor Manufacturing* 3 (4), 230–238 (November 1990).
68. Y. E. Park and K. D. Wise, "An MOS Switched-Capacitor Readout Amplifier for Capacitive Pressure Sensors," Proc., *IEEE Custom Integrated Circuits Conf.* (May 1983), pp. 380–384.
69. A. Selvakumar, N. Yazdi, K. Najafi, "A Low Power, Wide Range Threshold Acceleration Sensing System," Proc., *IEEE Microelectromechanical Systems Workshop* (San Diego, CA, February 1996), pp. 186–191.
70. J. L. Lund and K. D. Wise, "Chip-Level Encapsulation of Implantable CMOS Microelectrode Arrays," *Digest Solid-State Sensor and Actuator Workshop* (Hilton Head, June 1994 SC), pp. 29–32.

71. H. Guckel and D. W. Burns, "Planar Processed Polysilicon Sealed Cavities for Pressure Transducer Arrays," *Digest IEEE IEDM* (December 1984).
72. L. Spangler and C. Kemp, "ISAAC: Integrated Silicon Automotive Accelerometer," *Digest Int. Conf. on Solid-State Sensors and Actuators* (Stockholm, June 1995), pp. 585–588.
73. S. B. Crary, W. G. Baer, J.C. Cowles, and K. D. Wise, "Digital Compensation of High-performance Silicon Pressure Transducers," *Sensors and Actuators A* 21–23, 70–72 (1990).
74. S. B. Crary, L. Hoo, and M. Tennenhouse, "I-Optimality Algorithm and Implementation," *Proc., Symposium on Computational Statistics*, Vol. 2 (Neuchatel, Switzerland, August 1992), pp. 209–214.
75. G. Harvey, S. Louis, and S. Buska, "Micro-time stress measurement device development," Rome Laboratory technical report no. (ERSR), RL-TR-94-196 (November, 1994).